Centrality, rapidity, and transverse momentum dependence of isolated prompt photon production in lead-lead collisions at $\sqrt{s_{NN}} = 2.76$ TeV measured with the ATLAS detector

G. Aad *et al.**

(The ATLAS Collaboration)

Prompt photon production in $\sqrt{s_{NN}} = 2.76$-TeV Pb + Pb collisions has been measured by the ATLAS experiment at the Large Hadron Collider using data collected in 2011 with an integrated luminosity of 0.14 nb^{-1}. Inclusive photon yields, scaled by the mean nuclear thickness function, are presented as a function of collision centrality and transverse momentum in two pseudorapidity intervals, $|\eta| < 1.37$ and $1.52 \leqslant |\eta| < 2.37$. The scaled yields in the two pseudorapidity intervals, as well as the ratios of the forward yields to those at midrapidity, are compared to the expectations from next-to-leading-order perturbative QCD (pQCD) calculations. The measured cross sections agree well with the predictions for proton-proton collisions within statistical and systematic uncertainties. Both the yields and the ratios are also compared to two other pQCD calculations, one which uses the isospin content appropriate to colliding lead nuclei and another which includes nuclear modifications to the nucleon parton distribution functions.

I. INTRODUCTION

Prompt photons are an important probe for the study of the hot, dense matter formed in the high-energy collision of heavy ions. Being colorless, they are transparent to the subsequent evolution of the matter and probe the very initial stages of the collision. Their production rates are therefore expected to be directly sensitive to the overall thickness of the colliding nuclear matter. The rates are also expected to be sensitive to modifications of the partonic structure of nucleons bound in a nucleus, which are implemented as nuclear modifications [1–3] to the parton distribution functions (PDFs) measured in deep-inelastic lepton-proton and proton-proton (pp) scattering experiments. These effects include nuclear shadowing (the depletion of the parton densities at low Bjorken x), antishadowing (an enhancement at moderate x), and the EMC effect [4]. Photon rates are also sensitive to final-state interactions in the hot and dense medium, via the conversion of high-energy quarks and gluons into photons through rescattering. This is predicted to lead to an increased photon production rate relative to standard expectations [5,6].

Prompt photons have two primary sources. The first is direct emission, which proceeds at leading order via quark-gluon Compton scattering $qg \rightarrow q\gamma$ or quark-antiquark annihilation $\bar{q}q \rightarrow g\gamma$. The second is the fragmentation contribution from the production of hard photons during parton fragmentation. At leading order in perturbative quantum chromodynamics (pQCD) calculations, there is a meaningful distinction between the direct emission and fragmentation, but at higher orders the two cannot be unambiguously separated. To suppress the large background of nonprompt photons originating from the

decays of neutral mesons in jets, as well as fragmentation photons, an isolation criterion is applied, in both measurements and calculations, to the transverse energy contained within a cone of well-defined size around the photon direction [7]. The isolation transverse energy requirement can be applied as a fraction of the photon transverse energy or as a constant transverse energy threshold. In either case, these requirements can be applied consistently to pQCD calculations so that prompt photon rates can be calculated reliably, as the isolation criterion naturally cuts off the collinear divergence of the fragmentation contribution [7].

Prompt photon rates have been measured extensively in both fixed-target and collider experiments. Fixed-target experiments include WA70 [8], UA6 [9], and E706 [10], and cover the range $\sqrt{s} = 23$–38.8 GeV. In collider experiments, measurements were performed for proton-proton collisions at the CERN Intersecting Storage Rings (pp, $\sqrt{s} = 24$–62.4 GeV) [11,12], and BNL Relativistic Heavy Ion Collider (pp at $\sqrt{s} = 200$ GeV) [13,14], and for proton-antiproton collisions at the CERN Super Proton Synchrotron ($\bar{p}p$, $\sqrt{s} = 546$–630 GeV) [15,16] and at the Fermilab Tevatron ($\bar{p}p$, $\sqrt{s} = 0.63$–1.96 TeV) [17–20]. At the CERN Large Hadron Collider (LHC), ATLAS [21–23] and CMS [24,25] have measured isolated prompt photons in pp collisions at $\sqrt{s} = 7$ TeV. In most cases, good agreement has been found with pQCD predictions at next-to-leading order (NLO), which are typically calculated using the JETPHOX package [7,26]. In lower-energy heavy-ion collisions, the WA98 experiment observed direct photons in lead-lead (Pb + Pb) collisions at $\sqrt{s_{NN}} = 17.3$ GeV [27], and the PHENIX experiment performed measurements of direct photon rates in gold-gold collisions at $\sqrt{s_{NN}} = 200$ GeV [28,29].

A variable often used to characterize the modification of rates of hard processes in a nuclear environment is the nuclear modification factor,

$$R_{AA} = \frac{(1/N_{evt})dN_X/dp_T}{\langle T_{AA}\rangle d\sigma_X^{pp}/dp_T}, \tag{1}$$

---

*Full author list given at the end of the article.

where dN_X/dp_T is the yield of objects X produced in a p_T interval, N_{evt} is the number of sampled minimum-bias events, T_{AA} is the mean nuclear thickness function (defined as the mean number of binary collisions divided by the total inelastic nucleon-nucleon (NN) cross section), and $d\sigma_X^{pp}/dp_T$ is the cross section of process X in pp collisions for the same p_T interval. With this formula, one can make straightforward comparisons of yields in heavy-ion collisions, normalized by the flux of initial-state partons, to those measured in pp data, or calculated in pQCD. CMS performed the first measurement of isolated prompt photon rates in both Pb + Pb and pp collisions at $\sqrt{s} = 2.76$ TeV up to a photon transverse energy $E_T = 80$ GeV within $|\eta| < 1.44$ [30]. This measurement observed prompt, isolated photon rates consistent with $R_{AA} = 1$ for all collision impact parameters and E_T ranges considered, and good agreement of the data with JETPHOX calculations.

This paper presents isolated prompt photon yields, scaled by the mean nuclear thickness to derive effective cross sections, measured in Pb + Pb collisions with the ATLAS detector, making use of its large-acceptance, longitudinally segmented calorimeter system. The effect of the underlying event (UE) on the photon energy and shower shape is corrected on an event-by-event basis. Photon yields are measured over two ranges in the pseudorapidity of the photon, $|\eta| < 1.37$ (central) and $1.52 \leqslant |\eta| < 2.37$ (forward), and for photon transverse momenta in the interval $22 \leqslant p_T < 280$ GeV. Comparisons of the yields with NLO pQCD calculations are also presented from JETPHOX 1.3 [26], in three configurations: pp collisions, Pb + Pb collisions (i.e., with the correct total isospin), and Pb + Pb after incorporating the EPS09 nuclear modification factors to the nucleon PDFs [1], derived from experimental data of lepton and proton scattering on nuclei. The ratios of the yields in the forward η region to those in the central η region ($R_{FC\eta}$) are also presented.

II. ATLAS DETECTOR

The ATLAS detector comprises three major subsystems: the inner detector, the calorimeter system, and the muon spectrometer. It is described in detail in Ref. [31].

The inner detector is composed of the pixel detector, the semiconductor tracker (SCT), and the transition radiation tracker (TRT), which cover the full azimuthal range and pseudorapidities[1] $|\eta| < 2.5$, except for the TRT, which covers $|\eta| < 2$. The muon spectrometer measures muons over $|\eta| < 2.7$ with a combination of monitored drift tubes and cathode strip chambers.

The ATLAS calorimeter is the primary subsystem used for the measurement presented here. It is a large-acceptance, longitudinally segmented sampling calorimeter covering $|\eta| <$

---

[1] ATLAS uses a right-handed coordinate system with its origin at the nominal interaction point (IP) in the center of the detector and the z axis along the beam pipe. The x axis points from the IP to the center of the LHC ring, and the y axis points upward. Cylindrical coordinates (r, ϕ) are used in the transverse plane, ϕ being the azimuthal angle around the beam pipe. The pseudorapidity is defined in terms of the polar angle θ as $\eta = -\ln\tan(\theta/2)$.

4.9 with electromagnetic (EM) and hadronic sections. The EM section is a lead–liquid-argon sampling calorimeter with an accordion-shaped geometry. It is divided into a barrel region, covering $|\eta| < 1.475$, and two end-cap regions, covering $1.375 < |\eta| < 3.2$. The EM calorimeter has three primary sections, longitudinal in shower depth, called "layers," to fully contain photon showers in the range of interest for this analysis. The first sampling layer is 3 to 5 radiation lengths deep and is segmented into fine strips of size $\Delta\eta = 0.003$–0.006 (depending on η), which allows the discrimination of photons from the two-photon decays of π^0 and η mesons. The second layer is 17 radiation lengths thick, sampling most of an electromagnetic shower, and has cells of size $\Delta\eta \times \Delta\phi = 0.025 \times 0.025$. The third layer has a material depth ranging from 4 to 15 radiation lengths and is used to correct for the leakage beyond the first two layers for high-energy electromagnetic showers. The total material in front of the electromagnetic calorimeter ranges from 2.5 to 6 radiation lengths depending on pseudorapidity, except in the transition region between the barrel and end-cap regions ($1.37 \leqslant |\eta| < 1.52$), in which the material is up to 11.5 radiation lengths (for which reason this transition region is excluded from this analysis). In front of the strip layer, a presampler is used to correct for energy loss in front of the calorimeter within the region $|\eta| < 1.8$. In test beam environments and in typical pp collisions, the photon energy resolution is found to have a sampling term of 10%–17%/$\sqrt{E[\text{GeV}]}$. Above 200 GeV, the global constant term in the photon energy resolution, estimated to be $1.2\% \pm 0.6\%$ ($1.8\% \pm 0.6\%$) in the barrel (end-cap) region for pp data at $\sqrt{s} = 7$ TeV, starts to dominate [32]. The hadronic calorimeter section is located outside the electromagnetic calorimeter. Within $|\eta| < 1.7$, it is a sampling calorimeter of steel and scintillator tiles, with a depth of 7.4 hadronic interaction lengths.

The ATLAS zero-degree calorimeters (ZDCs) are used for minimum-bias event triggering. They detect forward-going neutral particles with $|\eta| > 8.3$. The minimum-bias trigger scintillators (MBTSs) detect charged particles in the interval $2.1 < |\eta| < 3.9$ using two sets of 16 counters positioned at $z = \pm 3.6$ m. They are used for event selection. The forward calorimeter (FCal) is used to determine the "centrality" of the collision, which can be related to geometric parameters such as the number of participating nucleons or the number of binary collisions [33]. The FCal has three layers in the longitudinal direction, one electromagnetic and two hadronic, covering $3.1 < |\eta| < 4.9$. The FCal electromagnetic and hadronic modules are composed of copper and tungsten absorbers, respectively, with liquid argon as the active medium, which together provide ten interaction lengths of material.

The sample of events used in this analysis was collected using the first-level calorimeter trigger [34]. This is a hardware trigger that sums the electromagnetic energy in towers of size $\Delta\eta \times \Delta\phi = 0.1 \times 0.1$. A sliding window of size 0.2×0.2 was used to find electromagnetic clusters by searching for local energy maxima and keeping only those clusters with energy in two adjacent towers (i.e., regions with a size of either 0.2×0.1 or 0.1×0.2) exceeding a threshold. The trigger used for the present measurement had a threshold of 16 GeV transverse energy.

TABLE I. Centrality bins used in this analysis, tabulating the percentage range, the average number of participants ($\langle N_{\mathrm{part}} \rangle$) and binary collisions ($\langle N_{\mathrm{coll}} \rangle$), the mean nuclear thickness ($\langle T_{\mathrm{AA}} \rangle$), and the relative systematic uncertainty on these quantities.

Interval (%)	$\langle N_{\mathrm{part}} \rangle$	$\frac{\delta \langle N_{\mathrm{part}} \rangle}{\langle N_{\mathrm{part}} \rangle}$ (%)	$\langle N_{\mathrm{coll}} \rangle$	$\frac{\delta \langle N_{\mathrm{coll}} \rangle}{\langle N_{\mathrm{coll}} \rangle}$ (%)	$\langle T_{\mathrm{AA}} \rangle$ (mb^{-1})	$\frac{\delta \langle T_{\mathrm{AA}} \rangle}{\langle T_{\mathrm{AA}} \rangle}$ (%)
0–10	356.2	0.7	1500.6	7.6	23.4	1.6
10–20	260.7	1.4	923.3	7.3	14.4	2.1
20–40	157.8	2.4	440.6	7.2	6.9	3.5
40–80	45.9	5.9	77.8	9.1	1.2	8.1

III. COLLISION DATA SELECTION

The data sample analyzed in this paper corresponds to an integrated luminosity of $\mathcal{L}_{\mathrm{int}} = 0.14 \, \mathrm{nb}^{-1}$ Pb + Pb collisions at $\sqrt{s_{NN}} = 2.76$ TeV collected during the 2011 LHC heavy-ion run. After the trigger requirement, events must satisfy a set of selection criteria. To suppress backgrounds, the relative time measured between the two MBTS counters is required to be less than 5 ns, and a primary vertex is required to be reconstructed in the inner detector. Minimum-bias events were triggered in the same data samples based on either a coincidence in the two ZDCs associated with a track in the inner detector, or a total of at least 50 GeV transverse energy deposited in the full calorimeter system. These events were also required to pass the same MBTS and vertex selections as the photon-triggered events. To be consistent with the minimum-bias trigger selections, a ZDC coincidence is also required for photon-triggered events with low FCal ΣE_{T}.

The centrality of each heavy-ion collision is determined using the total transverse energy measured in the forward calorimeter ($3.2 < |\eta| < 4.9$), at the electromagnetic scale, FCal ΣE_{T}. The trigger and event selection were studied in detail in the 2010 Pb + Pb data sample [35] and 98% ± 2% of the total inelastic cross section was accepted. The higher luminosity of the 2011 heavy-ion run necessitated a more sophisticated trigger strategy, including more restrictive triggers in the most peripheral events. However, it was found that the FCal ΣE_{T} distributions in 2011 data match those measured in 2010 to a high degree of precision. For this analysis, the FCal ΣE_{T} distribution was divided into four centrality intervals, covering the 0%–10%, 10%–20%, 20%–40%, and 40%–80% most central events. With this convention, the 0%–10% interval contains the events with the largest forward transverse energy production, and the 40%–80% interval the smallest. The total number of minimum-bias events corresponding to the 0%–80% centrality interval is $N_{\mathrm{evt}} = 7.93 \times 10^8$.

Quantities which describe the average geometric configuration of the colliding nuclei are calculated as described in Ref. [36] using a Glauber Monte Carlo calculation to describe the measured minimum-bias FCal distribution. Table I summarizes all of the centrality-related information used in this analysis. For each centrality interval, the table specifies the mean number of nucleons that interact at least once $\langle N_{\mathrm{part}} \rangle$, the mean number of binary collisions $\langle N_{\mathrm{coll}} \rangle$, and the mean value of the nuclear thickness function $\langle T_{\mathrm{AA}} \rangle$, with their respective fractional uncertainties. The uncertainty on the mean nuclear thickness function $\langle T_{\mathrm{AA}} \rangle = \langle N_{\mathrm{coll}} \rangle / \sigma_{NN}$ is smaller than the corresponding uncertainty on $\langle N_{\mathrm{coll}} \rangle$, because the uncertainty on σ_{NN} largely cancels in the ratio. All of

the uncertainties account for variations in the Glauber model parameters consistent with the uncertainties about the nuclear wave function, as well as the uncertainty in the estimation of the measured fraction of the total inelastic cross section.

Because the distribution of FCal ΣE_{T} is different in events with high-p_{T} photons compared to minimum-bias events, a weighting factor is applied to each simulated event to make the simulated distributions agree with the measured distributions.

IV. SIMULATED DATA SAMPLES

For the extraction of photon reconstruction and identification efficiencies, the photon energy scale, and expected properties of the isolation transverse energy distributions, samples of events containing prompt photons were produced using PYTHIA 6.423 [37] for pp collisions at $\sqrt{s} = 2.76$ TeV using the ATLAS AUET2B set of tuned parameters [38]. Direct photons were simulated in photon-jet events divided into four subsamples based on requiring a minimum p_{T} for the primary photon: $p_{\mathrm{T}} > 17$ GeV, $p_{\mathrm{T}} > 35$ GeV, $p_{\mathrm{T}} > 70$ GeV, and $p_{\mathrm{T}} > 140$ GeV. The contribution of fragmentation photons was modeled using a set of simulated inclusive-jet pp events, also using the same PYTHIA 6 tune. Each of these is required to have a hard photon produced in the fragmentation of jets produced with the PYTHIA 6 hardness scale, which controls the typical p_{T} of the produced jets, ranging from 17 to 560 GeV. Similar samples were also prepared using the SHERPA generator [39] using the CT10 [40] parton distribution functions, which include both direct and fragmentation photon contributions. These were used to check on the generator dependence of the photon efficiency. A large sample of PYTHIA 6 inclusive-jet events, without the hard photon requirement, were utilized to study the properties of background candidates. For all generated samples, each event was fully simulated using GEANT4 [41,42].

Each simulated event is overlaid upon a real minimum-bias event from experimental data, with the simulated event vertex placed at the position of the measured vertex position. By using minimum-bias data as the underlying-event model, almost all features of the underlying event are preserved in the simulation, including the full details of its azimuthal correlations.

A reconstructed photon is considered "matched" to a prompt generator-level ("truth") photon when they are separated by an angular distance $\Delta R = \sqrt{(\Delta \phi)^2 + (\Delta \eta)^2} < 0.2$. If multiple reconstructed photons are within the matching window, only the highest-p_{T} reconstructed photon is considered matched to the truth photon.

V. PHOTON RECONSTRUCTION

The electromagnetic shower associated with each photon, as well as the total transverse energy in a cone surrounding it, are reconstructed as described in Ref. [43]. However, in a heavy-ion collision, it is important to subtract the large UE from each event before the reconstruction procedure is applied. If it is not subtracted, photon transverse energies can be overestimated by up to several GeV in the most central events and the isolation transverse energy in a $\Delta R = 0.3$ cone can be overestimated by about 60 GeV. The procedure explained in Ref. [44] is used to estimate the energy density of the underlying event in each calorimeter cell. It iteratively excludes jets from consideration to obtain the average energy density in each calorimeter layer in intervals of $\Delta\eta = 0.1$, after accounting for the elliptic modulation relative to the event plane angle measured in the FCal [35,45]. The algorithm provides the energy density as a function of η, ϕ, and calorimeter layer, which allows the event-by-event subtraction of the UE in the electromagnetic and hadronic calorimeters.

After subtraction, the residual deposited energies stem primarily from three sources: jets, photons/electrons, and UE fluctuations (including higher-order flow harmonics). It should be noted that while this provides an estimate of the mean underlying transverse energy as a function of η, it is at present not possible to make further subtraction of more localized structures.

The ATLAS photon reconstruction [43] is seeded by clusters with $E_T > 2.5$ GeV found using a sliding-window algorithm applied to the second sampling layer of the electromagnetic calorimeter, which typically contains over 50% of the shower energy. In the dense environment of the heavy-ion collision, the photon conversion reconstruction procedure is not performed, owing to the large number of combinatoric pairs in more central collisions. However, a substantial fraction of converted photons is still reconstructed by the photon algorithm as, for high-energy photon conversions, the electron and positron are typically close together when they reach the calorimeter, while their tracks typically originate at a radius too large to be well described by the tracking algorithm that is used for heavy-ion collisions. Thus, the photon sample analyzed here is a mix of converted and unconverted photons. From simulations, the overall conversion rate is found to be about 30% in $|\eta| < 1.37$ and 60% in $1.52 \leqslant |\eta| < 2.37$.

The energy measurement is made using the three layers of the electromagnetic calorimeter and the presampler, with a window size corresponding to 3×5 cells (in η and ϕ) in the second layer in the barrel and 5×5 cells in the end-cap region. An energy calibration is applied to each shower to account for both its lateral leakage (outside the nominal window) and longitudinal leakage (into the hadronic calorimeter as well as dead material) [43]. For converted photons, this window size can lead to an underestimate of the photon candidate's energy, which is accounted for in the data analysis. The transverse energy of the photon is defined as the calibrated cluster energy multiplied by the sine of the polar angle determined with respect to the measured event vertex. The transverse momentum of the photon is identified with the measured transverse energy.

The fine-grained, longitudinally segmented calorimeter allows for a detailed characterization of the shape of each photon shower, which can be used to reject neutral hadrons while maintaining a high efficiency for photons. Nine shower shape variables are used for each photon candidate.

The primary shape variables used can be broadly classified by which sampling layer is used. The second sampling layer is used to measure the following.

   (i) R_η, the ratio of energies deposited in a 3×7 ($\eta \times \phi$) window to those deposited in a 7×7 set of cells in the second layer;

  (ii) R_ϕ, the ratio of energies deposited in a 3×3 ($\eta \times \phi$) window to those deposited in a 3×7 set of cells in the second layer;

 (iii) $w_{\eta,2}$, the standard deviation in the η projection of the energy distribution of the cluster in a 3×5 set of cells in the second layer.

The hadronic calorimeter is used to measure the fraction of shower energy that is detected behind the electromagnetic calorimeter. Only one of these is applied to each photon, depending on its pseudorapidity.

   (i) R_{had}, the ratio of transverse energy measured in the hadronic calorimeter to the transverse energy of the photon candidate (this quantity is used for $0.8 \leqslant |\eta| < 1.37$);

  (ii) R_{had1}, the ratio of transverse energy measured in the first sampling layer of the hadronic calorimeter to the transverse energy of the photon candidate (this quantity is used for photons with either $|\eta| < 0.8$ or $|\eta| \geqslant 1.52$).

Finally, cuts are applied to five other quantities, measured in the fine-granularity first layer, to reject neutral meson decays from jets. In this finely segmented layer a search for multiple maxima from electromagnetic decays of neutral hadrons is performed.

   (i) $w_{s,tot}$, the standard deviation of the energy distribution in the η projection in the first sampling "strip" layer, in strip cell units;

  (ii) $w_{s,3}$, the standard deviation of the energy distribution in three strips including and surrounding the cluster maximum in the strip layer, also in strip cell units;

 (iii) F_{side}, the fraction of energy in seven strips surrounding the cluster maximum, not contained in the three core strips;

 (iv) E_{ratio}, the asymmetry between the energies in the first and second maxima in the strip layer cells (this quantity is equal to one when there is no second maximum);

  (v) ΔE, the difference between the energy of the second maximum and the minimum cell energy between the first two maxima (this quantity is equal to zero when there is no second maximum).

In a previous ATLAS measurement [21], it was observed that the distributions of the shower-shaped variables measured in data differ systematically from those in the simulation. To
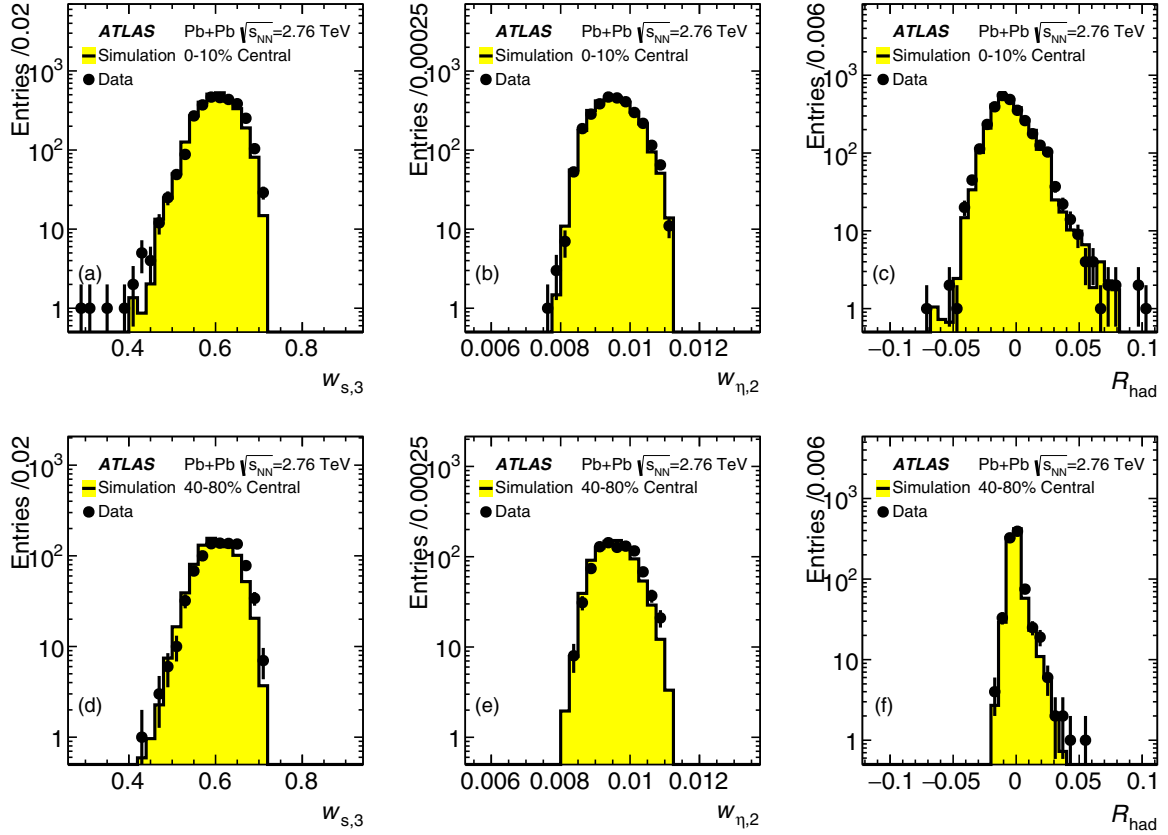
FIG. 1. Comparisons of distributions of three shower-shaped variables ($w_{s,3}$, $w_{\eta,2}$, and R_{had}) from data (black points) with simulation results after shower shape corrections (yellow histogram) for tight and isolated photons with reconstructed $35 \leqslant p_T < 44.1\,\mathrm{GeV}$ and $|\eta| < 1.37$. Events from the 0%–10% centrality interval are shown in the top row (a)–(c), while those from the 40%–80% interval are shown in the bottom row (d)–(f).

account for these differences, a set of correction factors was derived, each of which changes the value of a simulated shower shape variable such that its mean value matches that of the corresponding measured distribution. For the measurements presented in this paper, the same correction factors, obtained by comparing pp simulations to the same quantities in data, are used with no modification for the heavy-ion environment. They were validated in the heavy-ion environment using electrons and positrons from reconstructed $Z \rightarrow e^+e^-$ decays from the same LHC run. It was observed that the magnitude and centrality dependence of the mean values of the shape variables are well described by simulations, within the limited size of the electron and positron sample.

Figure 1 shows three typical distributions of shower shape variables for data from the 0%–10% and 40%–80% centrality intervals, each compared with the corresponding quantities in the simulation. The simulated distributions, after shower shape corrections, are all normalized to the number of counts in the corresponding data histogram. The data contain some admixture of neutral hadrons, so complete agreement should not be expected in the full distributions. The admixture of converted photons, which depends on the amount of material in front of the electromagnetic calorimeter, and thus the pseudorapidity of the photon, is not accounted for in the analysis, but there is good agreement of the shower shape variable distributions between data and simulation.

Converted photons tend to have wider showers than unconverted photons and so substantially broaden the shower shape variables.

The electromagnetic-energy-trigger efficiency was investigated using a sample of minimum-bias data, where the primary triggers did not select on particular high-p_T activity. Using these, the probability for photon candidates selected for this analysis to match a first-level trigger with $E_{T,trig} > 16\,\mathrm{GeV}$ and $\Delta R < 0.15$ exceeds 99% for well-reconstructed photon candidates with $p_T \geqslant 22\,\mathrm{GeV}$ and over the full centrality range. In the more central events, the underlying-event contribution to the photon candidate reduces the effective threshold down by several GeV relative to the more peripheral events. To work in the plateau region, the minimum p_T required in this analysis is 22 GeV.

Photons are selected for offline analysis using a variation of the "tight" selection criteria developed for the photon analysis in pp collisions [21], necessitated by the additional fluctuations in the shower shape variables induced by the underlying event in heavy-ion collisions. Specific intervals are defined for all nine shower shape variables and are implemented in a p_T-independent, but η-dependent scheme. The intervals for each variable are defined to contain 97% of the distribution of isolated reconstructed photons matched to isolated truth photons with a reconstructed p_T in the region $40 \leqslant p_T < 60\,\mathrm{GeV}$ in the 0%–10% centrality interval (where

the UE fluctuations are largest), using the isolation criteria described in the next section.

To derive a data-driven estimate of the background candidates from jets, a "nontight" selection criterion is defined, which is particularly sensitive to neutral hadron decays. For this selection, a photon candidate is required to fail at least one of four shower shape selections in the first calorimeter layer: $w_{s,3}$, F_{side}, E_{ratio}, and ΔE. These reversed selections enhance the probability of accepting neutral hadron decays from jets, via candidates with a clear double shower structure (via E_{ratio} and ΔE) as well as candidates in which the two showers may have merged (via $w_{s,3}$ and F_{side}) [21].

While the photon energy calibration is the same as used for pp collisions, based in part on measurements of Z bosons decaying into an electron and a positron, and validated with $Z \rightarrow \ell\ell + \gamma$ events [46], the admixture of converted and unconverted photons leads, on average, to a small underestimate of the photon energy in Pb + Pb events, because the energies of converted photon clusters is typically reconstructed in a larger region in the calorimeter. This is quantified in the simulation by the mean fractional difference between the reconstructed and the truth photon transverse momenta $(p_T^{reco} - p_T^{truth})/p_T^{truth} \equiv \Delta p_T/p_T^{truth}$, obtained from simulation. For matched photons, the average deviation from the truth photon p_T is the largest at low photon p_T and is typically within 1% for $p_T > 44$ GeV. The fractional energy resolution, determined by calculating the standard deviation of the same quantity in smaller intervals in p_T^{truth}, ranges from 4.5% for $22 \leqslant p_T^{truth} < 26$ GeV to 1.5% for $p_T^{truth} = 200$ GeV for $|\eta| < 1.37$ and from 6% to 3% for $1.52 \leqslant |\eta| < 2.37$. The effects of energy scale and resolution are corrected for by using bin-by-bin correction factors described below.

The isolation transverse energy E_T^{iso} is the sum of transverse energies in calorimeter cells (including hadronic and electromagnetic sections) in a cone of size ΔR_{iso} around the photon direction. The photon energy is removed by excluding a central core of cells in a region corresponding to 5×7 cells in the second layer of the EM calorimeter. The cone size is chosen to be $\Delta R_{iso} = 0.3$, to reduce the sensitivity to UE fluctuations. The isolation criterion is $E_T^{iso} < 6$ GeV. An additional correction, based on simulations and parametrized primarily by the photon energy and η, is then applied to the calculated isolation transverse energy to minimize the effects of photon shower leakage into the isolation cone. It typically amounts to a few percent of the reconstructed photon transverse energy.

The left column of Fig. 2 shows the distributions of E_T^{iso} for tight photon candidates with $35 \leqslant p_T < 44.1$ GeV as a function of collision centrality, compared with simulated distributions. The data and simulations are normalized so the integrals of $E_T^{iso} < 0$, where no significant background from jet events is expected, are the same. Both, the simulated and the measured E_T^{iso} distributions grow noticeably wider with increasing centrality; as the UE subtraction only accounts for the mean energy in an η interval, local fluctuations are still present. Furthermore, in the data, an enhancement in events with $E_T^{iso} > 0$ is expected from the jet background. The E_T^{iso} distribution for a sample enhanced in backgrounds is shown in the right column of Fig. 2, which shows the isolation
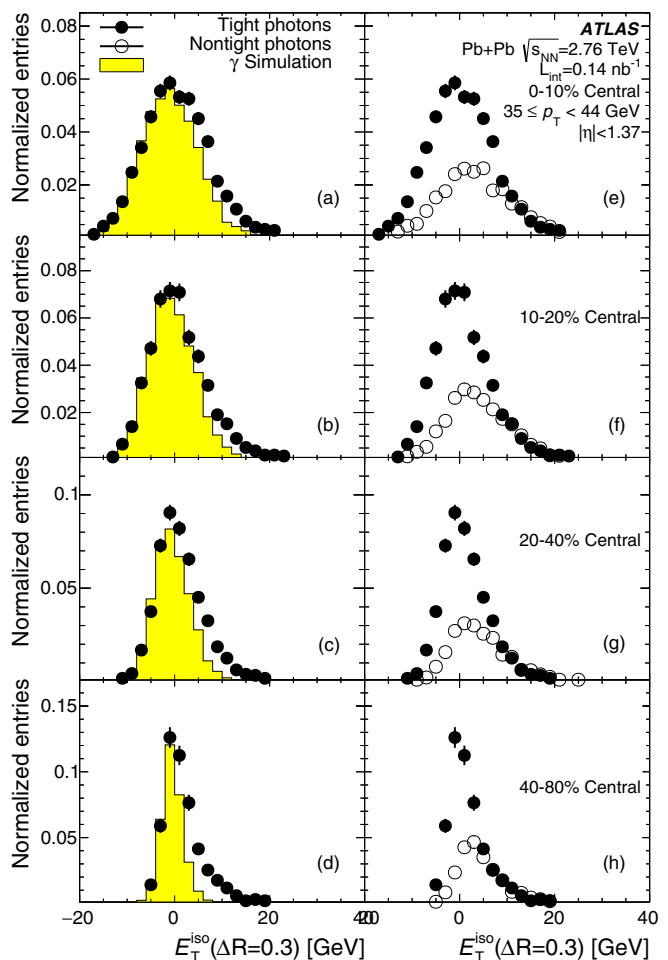

FIG. 2. Distributions of photon isolation transverse energy in a $\Delta R_{iso} = 0.3$ cone for the four centrality bins in data (black points, normalized by the number of events and by the histogram bin width) for photons with $35 \leqslant p_T < 44.1$ GeV. In the left column (a)–(d) simulations (yellow histogram) are normalized to the data so that the integrals in the range $E_T^{iso} < 0$ are the same. The corresponding sample of nontight photon candidates, normalized to the distribution of tight photons for $E_T^{iso} \geqslant 8$ GeV is shown overlaid on the tight photon data in the right column (e)–(h) to illustrate the source of the photons with large E_T^{iso}.

distribution for the nontight candidates in the same p_T interval. For larger values of E_T^{iso}, the distributions from the tight and nontight samples have similar shapes. The distributions are normalized to the integral of the tight photon candidate distribution in the region $E_T^{iso} > 8$ GeV.

After applying the tight selection and an isolation criterion of $E_T^{iso} < 6$ GeV to the 0%–80% centrality sample, there are 62 130 candidates with $p_T \geqslant 22.0$ GeV within $|\eta| < 1.37$ and 30 568 candidates within $1.52 \leqslant |\eta| < 2.37$.

VI. YIELD EXTRACTION

The kinematic intervals used in this analysis are defined as follows. For each centrality interval, as described in Sec. III, the photon kinematic phase space is divided into intervals in photon η and p_T. The two primary regions in η are $|\eta| < 1.37$
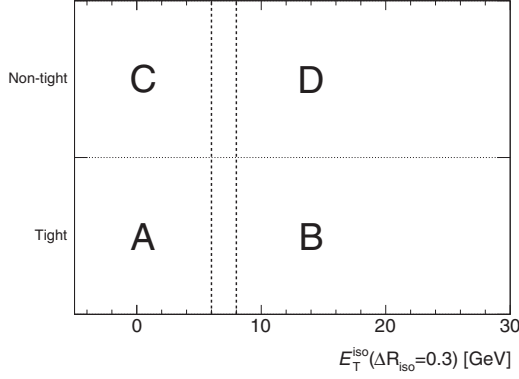
FIG. 3. Illustration of the double-sideband approach, showing the two axes for partitioning photon candidates: region A is the "signal region" (tight and isolated photons); region B contains tight, nonisolated photons, region C contains nontight isolated photons; and region D contains nontight and nonisolated photons.

("central η") and $1.52 \leqslant |\eta| < 2.37$ ("forward η"). The p_T intervals used are logarithmic and are $17.5 \leqslant p_T < 22$ GeV (only used in simulations), $22.0 \leqslant p_T < 27.8$ GeV, $27.8 \leqslant p_T < 35.0$ GeV, $35.0 \leqslant p_T < 44.1$ GeV, $44.1 \leqslant p_T < 55.6$ GeV, $55.6 \leqslant p_T < 70.0$ GeV, $70.0 \leqslant p_T < 88.2$ GeV, $88.2 \leqslant p_T < 140$ GeV, and $140 \leqslant p_T < 280$ GeV.

Prompt photons are defined as photons produced in the simulation of the hard process, either directly or radiated from a primary parton, via a truth particle-level isolation transverse energy selection of $E_T^{iso} < 6$ GeV. The truth-level E_T^{iso} is defined using all final-state particles except for muons and neutrinos in a cone of $\Delta R = 0.3$ around the photon direction. To account for the underlying event in the hard process, the mean energy density is estimated for each simulated event using the jet-area method described in Ref. [21].

For each interval in p_T, η, and centrality ($\mathcal{C}$), the per-event yield of photons is defined as

$$\frac{1}{N_{evt}(\mathcal{C})} \frac{dN_\gamma}{dp_T}(p_T, \eta, \mathcal{C}) = \frac{N_A^{sig} \mathcal{U}(p_T, \eta, \mathcal{C}) \mathcal{W}(p_T, \eta, \mathcal{C})}{N_{evt}(\mathcal{C}) \epsilon_{tot}(p_T, \eta, \mathcal{C}) \Delta p_T}, \quad (2)$$

where N_A^{sig} is the background-subtracted yield, $\mathcal{U}$ is a factor that corrects for the bin migration owing to the photon energy resolution and any residual bias in the photon-energy scale, $\mathcal{W}$ is a factor that corrects for electron contamination from W and Z bosons, ϵ_{tot} is the combined photon reconstruction and identification efficiency, N_{evt} is the number of minimum-bias events in centrality interval $\mathcal{C}$, and Δp_T is the width of the transverse momentum interval.

The technique used to subtract the background from jets from the measured yield of photon candidates is the "double sideband" method, used in Refs. [21–23]. In this method, photon candidates are partitioned along two dimensions, illustrated in Fig. 3. The four regions are labeled A, B, C, and D and correspond to the four categories expected for reconstructed photons and background candidates.

(i) A, tight, isolated photons: signal region for prompt, isolated photons;

(ii) B, tight, nonisolated photons: a region expected to contain nonisolated photons produced in the vicinity of a jet or an upward UE fluctuation, as well as hadrons from jets with shower shapes similar to those of a tight photon;

(iii) C, nontight, isolated photons: a region containing isolated neutral hadron decays, e.g., from hard-fragmenting jets, as well as real photons that have a shower shape fluctuation that fails the tight selection;

(iv) D, nontight, nonisolated photons: a region populated by neutral hadron decays within jets, but which have both a small admixture of photons that fail the tight selection and are accompanied by a local upward fluctuation of the UE.

The nontight and nonisolated photons are used to estimate the background from jet events in signal region A. This is appropriate provided there is no correlation between the axes for background photon candidates, e.g., that the probability of a neutral hadron decay satisfying the tight or nontight selection criteria is not dependent on whether it is isolated. This was studied using a sample of high-p_T photon candidates from the large sample of PYTHIA inclusive-jet events. Possible correlations, parametrized by the R_{bkg} ratio [21], $R_{bkg} = N_A^{bkg} N_D^{bkg} / (N_B^{bkg} N_C^{bkg})$, are taken as a systematic uncertainty, as discussed in Sec. VII.

If there is no leakage of signal from region A to the other nonsignal regions (B, C, and D), the double-sideband approach utilizes the ratio of counts in C to D to extrapolate the measured number of counts in region B to correct the measured number of counts in region A, i.e.,

$$N^{sig} = N_A^{sig} = N_A^{obs} - N_B^{obs} \frac{N_C^{obs}}{N_D^{obs}}. \quad (3)$$

Leakage of signal into the background regions needs to be removed before attempting to extrapolate into the signal region. A set of "leakage factors" c_i is calculated to extrapolate the number of signal events in region A into the other regions. The leakage factors are calculated using the PYTHIA simulations in intervals of reconstructed photon p_T as $c_i = N_i^{sig} / N_A^{sig}$, where N_A^{sig} is the number of simulated tight, isolated photons. In the 40%–80% centrality interval, for $|\eta| < 1.37$ and for $22 \leqslant p_T < 280$ GeV, c_B is generally less than 0.01, c_C ranges from 0.09 to 0.02, and c_D is less than 0.003. In the 0%–10% centrality interval and over the same p_T range, c_B ranges from 0.08 to 0.11, c_C ranges from 0.13 to 0.04, and c_D is O(1%) or less. Except for c_B, which reflects the different isolation distributions in peripheral and central events, the leakage factors are of similar magnitude to those derived in the pp data analysis [21].

Including these factors and the correlation parameter R_{bkg}, the formula becomes

$$N_A^{sig} = N_A^{obs} - R_{bkg} (N_B^{obs} - c_B N_A^{sig}) \frac{(N_C^{obs} - c_C N_A^{sig})}{(N_D^{obs} - c_D N_A^{sig})}. \quad (4)$$

Equation (4) is solved for the yield of signal photons N_A^{sig}, with R_{bkg} assumed to be 1.0. The statistical uncertainties in the number of signal photons for each centrality, η, and
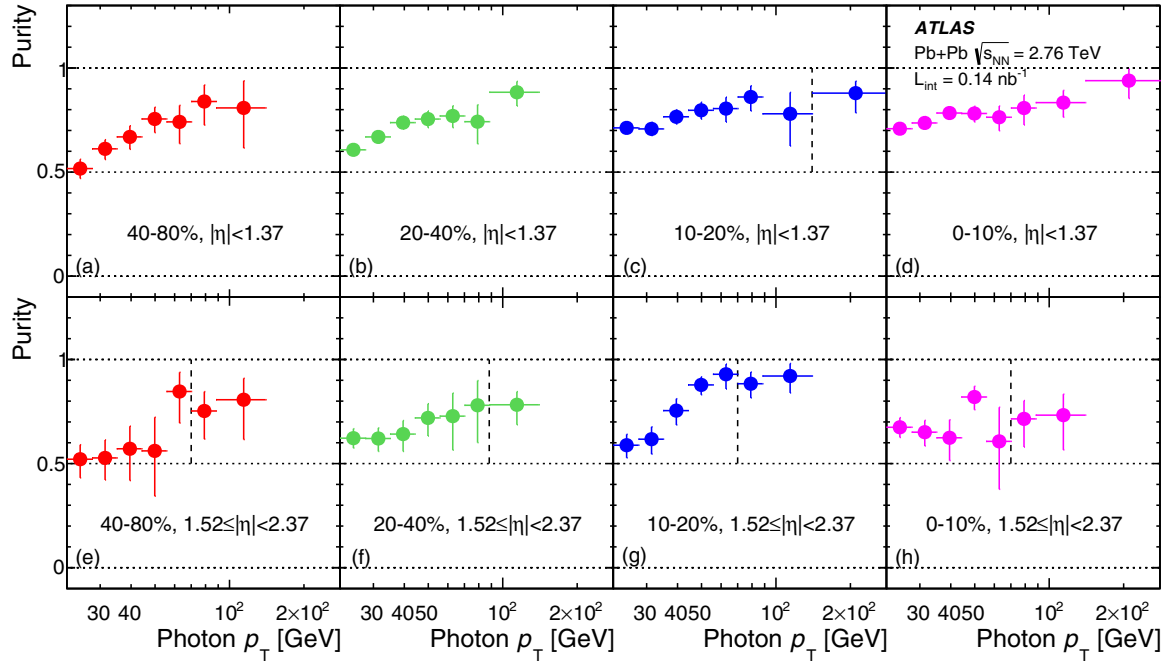
FIG. 4. Photon purity as a function of collision centrality (left to right) and photon p_T for photons measured in $|\eta| < 1.37$ [(a)–(d)] and $1.52 \leqslant |\eta| < 2.37$ [(e)–(h)]. The p_T intervals to the right of the vertical dotted line indicated in some bins use the extrapolation method described in the text to account for low event counts in the sidebands.

p_T interval are evaluated with 5000 pseudoexperiments. For each pseudoexperiment, the parameters N_A^{obs}, N_B^{obs}, N_C^{obs}, and N_D^{obs} are sampled from a multinomial distribution with the probabilities given by the observed values divided by their sum. The values of N_A^{sig}, N_B^{sig}, N_C^{sig}, and N_D^{sig} used to determine the leakage factors in each experiment, are themselves sampled from a Gaussian distribution with the parameters determined by the means of the simulated distributions and their statistical uncertainties. Pseudoexperiments where the leakage correction is negative are discarded to exclude trials where the extracted yield is larger than N_A^{obs}. The standard deviation of the distribution of N_A^{sig} obtained from the set of pseudoexperiments is taken as the statistical uncertainty.

The purity of the photon sample in the double-sideband method is then defined as $P = N_A^{\mathrm{sig}}/N_A^{\mathrm{obs}}$. The extracted values of P are shown in Fig. 4 as a function of transverse momentum in the four measured centrality intervals and two η intervals. In all four centrality and both η intervals, the purity increases from about 0.5 at the lowest p_T interval to 0.9 at the highest p_T intervals, with typically lower values in the forward η region. The statistical uncertainty in the purity is determined specifically using the pseudoexperiments described above, and by using the boundaries defined by the highest and lowest 16% of the purity distributions to determine the upper and lower asymmetric error bars.

For kinematic regions in which the number of candidates in the sidebands are small, particularly at the highest p_T values, the population of those sidebands are reestimated using a data-driven approach. For this, the ratio of each sideband (B, C, and D) to region A as a function of p_T is measured and extrapolated linearly in $1/p_T$, utilizing all of the available data up to $p_T = 140$ GeV. It should be noted that the purity merely represents the outcome of the sideband subtraction procedure and is not used as an independent correction factor. The several points for which this extrapolation is utilized are those to the right of the vertical dotted line in several of the Fig. 4 centrality intervals.

The reconstruction efficiency is the fraction of tight, isolated photons matched to the truth photons defined above ($E_T^{\mathrm{iso}} < 6$ GeV), according to the criterion specified in Sec. IV. The true photon p_T is used in the numerator and the denominator, while the reconstructed η is used in the numerator to estimate the very small inflow and outflow of photons in the large η intervals used in the analysis. The total efficiency can be factorized into the product of three contributions.

(i) Reconstruction efficiency: the probability that a photon is reconstructed with a p_T greater than 10 GeV. In the reconstruction algorithm, the losses primarily stem from a subset of photon conversions, for which the photon is reconstructed as an electron ("photon to electron leakage"). The losses are typically 5% near $\eta = 0$ and increase to about 10% at forward angles and are found to be approximately constant as a function of transverse momentum and centrality.

(ii) Identification efficiency: the probability that a reconstructed photon passes the tight identification selection criteria.

(iii) Isolation efficiency: the probability that a photon that would be reconstructed and pass the identification selection criteria also passes the chosen isolation selection. The large fluctuations from the UE in heavy-ion collisions can lead to a photon being found in the nonisolated region.
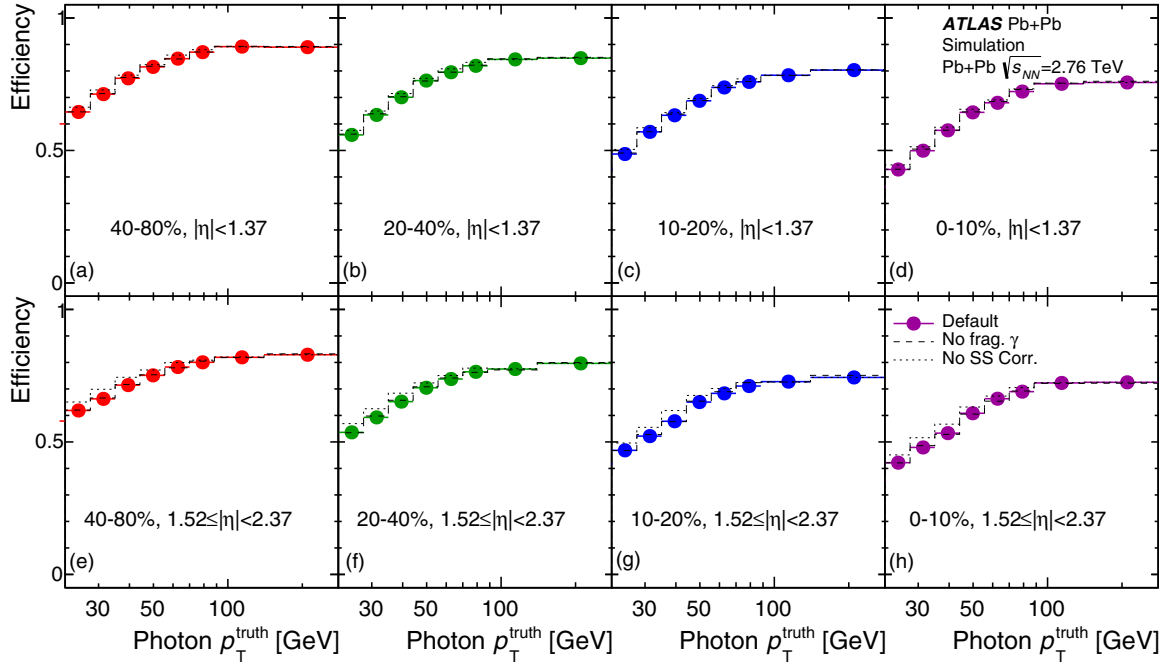
FIG. 5. Total photon efficiency as a function of photon p_T and event centrality averaged over $|\eta| < 1.37$ [(a)–(d)] and $1.52 \leqslant |\eta| < 2.37$ [(e)–(h)]. Variations of the efficiency from removing the small corrections to the simulated shower-shape variable, and from removing fragmentation photons from the simulations are shown by dotted and dashed lines, respectively.

Figure 5 shows the total efficiency for each centrality and η interval as a function of photon p_T. The primary systematic uncertainties on the efficiency were evaluated by removing the small correction factors applied to the simulated shower shapes and by excluding fragmentation photons from the sample used to derive the efficiencies. The contribution from each individual shower-shape selection is small, and so the effect on the efficiency is typically small, but the cumulative effect is as large as 10% in the lowest p_T intervals in the forward η region. Similar correction factors were calculated using the SHERPA simulations, and they are found to be consistent with the PYTHIA calculations in all considered centrality and η regions.

To account for the residual deviations of the measured photon p_T from the true p_T, stemming primarily from converted photons treated as unconverted, and from the photon energy resolution, the data are corrected using a bin-by-bin correction technique [21] to generate the correction factors $\mathcal{U}$. For each interval in centrality and η, a response matrix is formed by correlating the reconstructed p_T with the truth p_T for truth-matched photons. The projections onto each p_T interval along the truth axis T_i and the reconstructed axis R_i are then constructed for each centrality and η interval and their ratio $C_i = T_i/R_i$ is formed to calculate the correction in the corresponding p_T interval. To reduce the effect of statistical fluctuations, the C_i values were fit to a smooth functional form before applying to the data, with the deviations of the extracted correction factors from the fit being generally O(1%). In the lowest p_T interval ($22.1 \leqslant p_T < 28$ GeV), the correction factors deviate from unity by $+(6–9)\%$ in the central η region and $+(8–13)\%$ in the forward η region (the first number for the 40%–80% centrality interval and the second

for the 0%–10% interval). They approach unity rapidly as a function of p_T and in the highest p_T interval are -2% in the central η region and $+2\%$ in the forward η region. The reconstructed spectral shapes were compared between simulation and data and were found to agree within statistical uncertainties. Thus, no reweighting of the simulated spectrum was performed before calculating the bin-by-bin factors.

Samples of simulated W and Z bosons decaying to electrons or positrons, based on POWHEG [47] interfaced to the PYTHIA8 generator (version 8.175) [48], were used to study the estimated contamination rate relative to the total photon rates expected from JETPHOX). The raw contamination electron rates were corrected using the photon total efficiency. The difference in the extracted cross section of contamination electrons between the most peripheral and the most central events was found to be modest. Therefore, the centrality dependence is neglected and the cross sections calculated for the most central events are used in all centrality intervals. Based on this study, it was estimated that the largest background of the W and Z background is expected in the $35 \leqslant p_T < 44.1$ GeV interval with a magnitude of about 8% in the forward pseudorapidity region, and about 5% in the central region. In other bins the correction is smaller, and in most bins it is less than 2% in the central η region and less than 3% in the forward η region.

VII. SYSTEMATIC UNCERTAINTIES

The following systematic uncertainties are accounted for in this analysis. They are broadly classified into uncertainties that affect the efficiency, those that affect the yield extraction, and several other additional effects.

The systematic uncertainties that primarily affect the total efficiency are as follows.

(i) Photon-to-electron leakage: The misidentification of photons as electrons, owing to conversions, was studied using a sample simulated with extra material, and is found to be less than a 1% effect on the reconstruction efficiency, because these photons are considered unrecoverable.

(ii) Shower shape corrections: To assess the cumulative effect of the small shower shape corrections applied to mitigate the differences between data and simulation, the corrections are removed and the difference in the recalculated yields taken as a conservative systematic uncertainty. This is a smaller effect at higher p_T but is as large as 9% at low p_T in the forward η region.

(iii) Isolation criteria: To assess the impact of differences between the underlying E_T^{iso} distributions in data and simulation, several changes in the isolation selection were made. In one case, the cone size was changed to $\Delta R_{iso} = 0.4$ and the E_T^{iso} selection enlarged to 10 GeV. In the second, the E_T^{iso} selection was varied up and down by 2 GeV. Finally, the gap along the E_T^{iso} axis between regions A/C and B/D was removed. In all of these cases, the selections were similarly adjusted in simulation. In general, the variations in the yields show only a weak dependence on p_T. To reduce the effect of statistical fluctuations, the variations as a function of p_T are fit to constants over $22 \leqslant p_T < 44.1$ GeV and $44.1 \leqslant p_T < 140$ GeV, and the most significant variation is applied symmetrically to all points in that p_T region. If the fit value is consistent with zero, then the variation is reduced by half to avoid overcounting the statistical fluctuations. For the forward-central ratios, the variations are fit with a single function over $22 \leqslant p_T < 70$ GeV. In several cases, changing the isolation selection led to O(10%) changes that were clearly consistent with statistical fluctuations. In these cases, the variation was reduced to be 5%, similar to the adjacent centrality interval.

The shower leakage corrections were varied by 1% of the measured photon p_T in data, but not in simulation, to account for possible defects in the correction.

(iv) Fragmentation contribution: Excluding the fragmentation photons from the simulation sample has typically less than a 2% effect on the final yields over the full p_T range.

The systematic uncertainties that primarily affect the purity of the photon sample in each kinematic and centrality interval are as follows.

(i) Leakage factors: To test the sensitivity to mismodeling of the shower fluctuations that lead to leakage into sideband regions C and D, the leakage factors were conservatively varied up and down by 50%. The magnitude is given by the difference between the leakage factors in the 40%–80% peripheral events, where the underlying event does not cause large extra fluctuations, and the 0%–10% most central events.

This leads to up to 10% variations at low p_T, while the effect at higher p_T is below 5%.

(ii) Nontight definition: To assess the sensitivity to the choice of nontight criteria, which allow background into the analysis, the nontight definition was changed from four reversed conditions, to five (adding $w_{s,tot}$) and two (using just F_{side} and $w_{s,3}$). Similar to isolation criteria variations, fits to constant values in two p_T intervals (and one interval for the forward-central ratios) were performed to smoothen the bin-to-bin statistical fluctuations. In the central η interval, the variation is typically less than 5%, while it is 7% or less in the forward η interval.

(iii) Correlation of tight and isolation axes: The large inclusive-jet PYTHIA samples were used to study possible correlations between the tight selection criteria and the isolation transverse energy. This is characterized by calculating R_{bkg} for the backgrounds from jets, where the candidate is not matched to a truth photon. After integrating over centrality and p_T, R_{bkg} was found to vary by about 10% in the central η region and 20% in the forward η region, albeit with large statistical uncertainties. A conservative variation of $\pm 20\%$ was propagated through the analysis, which gives up to a 20% change at low p_T, where the purity is lowest, decreasing to typically less than 10% at higher p_T.

Uncertainties that pertain to corrections on the energy scale, electron contamination, and centrality are described here.

(i) Energy scale and resolution corrections: The effect of the energy scale and resolution from variations in material, different energy calibration schemes, and known differences between data and simulations in pp collisions are propagated into the bin-by-bin correction factors. The overall variation from the known sources is typically found to be below 2%–3%, and is approximately constant in p_T, but grows at high p_T in the forward η region. However, the extramaterial sample shows a small, but systematic, overall shift in the reconstructed energy scale which is approximately independent of p_T and centrality, but is larger in the forward η interval. Based on this, an overall uncertainty of 5% is assigned in the central η region and in the forward region, except in the forward region above 88.2 GeV, where 7% is assigned. In the ratio, these errors are treated as fully uncorrelated between the two η regions.

(ii) Electron contamination: The contamination from W and Z bosons was estimated to be largest in the two p_T intervals between 35 and 55.6 GeV and smaller in the other p_T intervals. Because the calculation does not account for the different expected leakage of the electrons into the different sidebands, and because the number of Z bosons in the heavy-ion data is too low to determine this fully, 50% of the contamination has been assigned as an uncertainty, leading to a maximum

TABLE II. Relative systematic uncertainties, expressed as a percentage, on the efficiency-corrected yields for selected p_T and centrality intervals in the two η intervals.

η	$\|\eta\| < 1.37$				$1.52 \leqslant \|\eta\| < 2.37$			
Centrality	40%–80%		0%–10%		40%–80%		0%–10%	
p_T (GeV)	22–28	55.6–70	22–28	70–88.2	22–28	55.6–70	22–28	70–88.2
$\gamma \rightarrow e$ leakage	1	1	1	1	1	1	1	1
Shower shape corr.	3	2	5	3	6	2	9	3
Isolation	7	5	6	8	6	10	5	9
Frag. photons	<1	<1	1	2	1	<1	2	2
Leakage factors	10	4	12	9	7	1	15	10
Nontight criteria	4	4	3	3	7	6	6	5
R_{bkg}	21	7	13	6	20	4	15	11
Energy scale	5	5	5	5	5	5	5	5
W/Z contamination	<1	1	<1	1	1	1	1	1
Cent. weight	4	1	1	<1	3	1	4	<1
η leakage	<1	<1	<1	<1	2	1	2	2
Total [%]	26	12	21	15	25	14	25	19

of 4% in one p_T interval in the forward region and smaller in all other intervals.

(iii) Centrality: The uncertainty on $\langle T_{AA} \rangle$ for each centrality interval is given in Table I and is shared by all p_T and η intervals for that centrality interval. In addition, the effect of reweighting the simulated FCal distribution generally has a less than 2% effect on the final yields, although the impact can increase to up to 4% at low p_T in the forward η interval.

(iv) η leakage: To address the effect of photons migrating in and out of the large η intervals when calculating the efficiency, the true η was also used for the efficiency calculations and was found to have a 1%–2% overall effect, reaching the larger end of this range in the forward η region.

For the absolute yields, all contributions are added in quadrature. For $R_{FC\eta}$, the systematic variations are performed based on the ratio of the forward and central η intervals after each variation to account for correlations between the two η regions. Thus, several of the effects discussed above, particularly the influence of the variations in the identification and isolation selection, partially cancel.

In the central η region, the uncertainties at lower p_T range from 18% to 26%, and those at higher p_T range from 8% to 16%. In the forward η region, the uncertainties at lower p_T range from 20% to 26%, and those at higher p_T range from 13% to 19%. For the yields, uncertainties for specific centrality, η and p_T ranges are provided in Table II. For the ratio $R_{FC\eta}$, the uncertainties at lower p_T range from 8% to 17% and at higher p_T from 6% to 12%. Uncertainties for specific centrality, η and p_T ranges are provided in Table II. For the ratios, uncertainties for specific centrality and p_T ranges are provided in Table III.

VIII. THEORETICAL PREDICTIONS

JETPHOX 1.3 is used for NLO pQCD calculations to compare with the fully corrected measurements. JETPHOX was found

to agree well (within 10%–15%) with $\bar{p}p$ from the Tevatron [19,20] and pp data from the LHC [21–23]. It provides access to a wide range of existing PDF sets and performs calculations for direct photon production as well as for photons from fragmentation processes, both using an implementation of the experimental isolation selection built into the calculations. The primary pp calculations shown in this work use the CTEQ6.6 [49] proton PDF, with no nuclear modification, and the BFG II fragmentation functions [50]. They require less than 6 GeV isolation energy in a cone of $\Delta R_{iso} = 0.3$ relative to the photon direction. The effect of hadronization on the final cross sections was estimated using the PYTHIA6.423 simulations to be 1% or less and is neglected in the results shown here. Scale uncertainties are estimated by varying the renormalization (μ_R), factorization (μ_F), and fragmentation (μ_f) scales by a factor of two, relative to the baseline result, $\mu_R = \mu_F = \mu_f = p_T^{photon}$. Two types of variations are performed, a correlated

TABLE III. Relative systematic uncertainties, expressed as a percentage, on the ratio of the yields in the forward η region and those in the central η region $R_{FC\eta}$ for selected p_T and centrality intervals in the two η intervals.

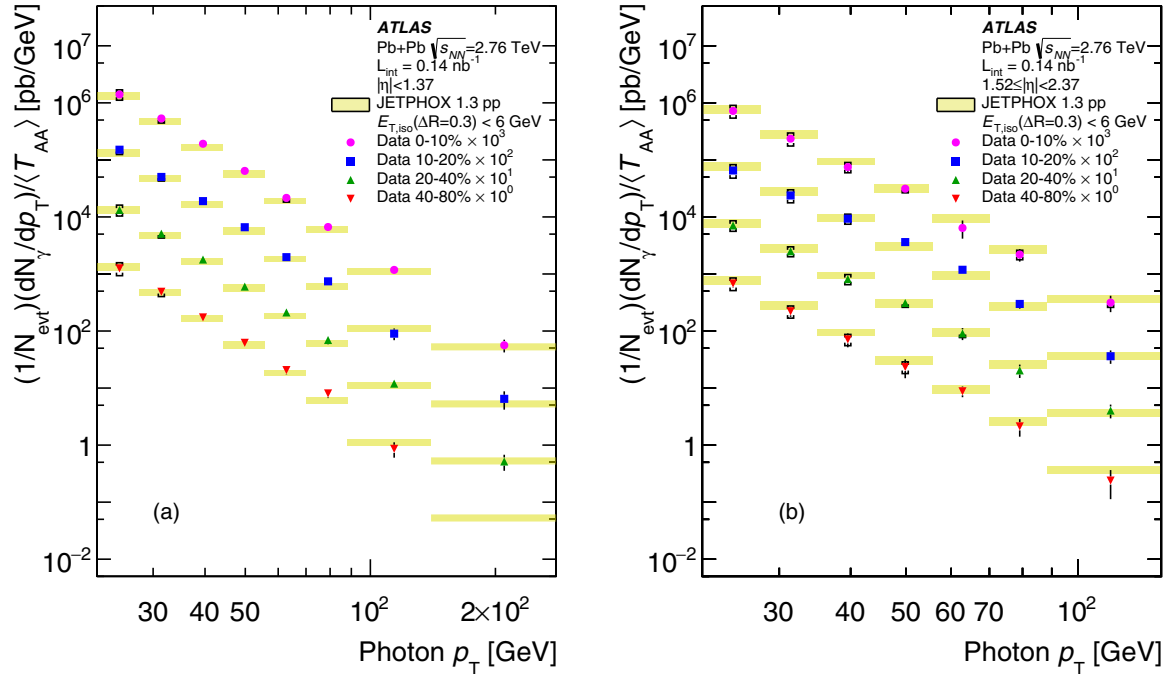| Centrality	40%–80%		0%–10%	
p_T (GeV)	22–28	55.6–70	22–28	70–88.2
$\gamma \rightarrow e$ leakage	1	1	1	1
Shower shape corr.	3	0	4	0
Isolation	9	9	4	4
Frag. photons	1	0	1	1
Nontight criteria	3	3	4	4
Leakage factors	2	2	2	4
R_{bkg}	1	4	2	6
Energy scale	7	7	7	7
W/Z contamination	0	1	0	1
Cent. weight	1	0	4	1
η leakage	2	1	2	2
Total (%)	13	13	11	11

FIG. 6. Fully corrected yields of prompt photons in four centrality intervals as a function of p_T in $|\eta| < 1.37$ (a) and $1.52 \leqslant |\eta| < 2.37$ (b) using tight selection, isolation cone size $\Delta R_{iso} = 0.3$, and isolation transverse energy of less than 6 GeV. JETPHOX calculations, for proton-proton collisions and using the same isolation criterion, are shown by the yellow bands. Statistical uncertainties are shown by the error bars. Systematic uncertainties on the photon yields are shown by braces, which are smaller than the markers for some points. The scale uncertainties owing to $\langle T_{AA} \rangle$ are tabulated for each bin in Table I.

variation of all three scales by a factor of two up and down, as well as an independent variation of each scale up and down by a factor of two, leaving the other two scales constant. The envelope covered by these variations is typically 12%–18%, varying with η and p_T. PDF uncertainties are determined by varying the PDF fit parameters according to 22 eigenvectors in the parameter space and separately keeping track of the upward and downward variations of the final cross sections. These uncertainties are generally less than 3% for $p_T < 100$ GeV but increase to 6% for pp for $p_T > 140$ GeV. The impact of the uncertainty in the strong coupling constant $\alpha_s(M_Z)$, $\Delta\alpha_s = \pm 0.0012$, was determined and found to be small. For

the yields it varies from $\pm(1–2)\%$, decreasing with p_T. For the ratio, it increases with p_T from 0 to 2.5%. These errors are not incorporated in the error bands shown. The calculations were also performed with the MSTW2008 PDF [51], which yield cross sections about 6% higher for $|\eta| < 1.37$ for all calculated p_T values.

To study nuclear effects, two additional calculations are performed. The first reweights the contributions from up and down valence quarks to account for the neutrons in the colliding lead nuclei, but with no attempt at modeling the impact parameter dependence of the neutron spatial distributions, e.g., owing to a neutron skin. This is a reasonable first-order approximation

TABLE IV. $\langle T_{AA} \rangle$-scaled prompt photon yields compared with JETPHOX 1.3 pp, for $|\eta| < 1.37$ in four centrality intervals and for JETPHOX as a function of photon p_T. For each value, the first uncertainty is statistical and the second is systematic. For JETPHOX, the combined error is shown.

p_T (GeV)	Scale	dN/dp_T / $\langle T_{AA} \rangle$ (pb/GeV)				$d\sigma/dp_T$ (pb/GeV)
		40%–80%	20%–40%	10%–20%	0%–10%	JETPHOX
22–28	10^3	$1.26 \pm 0.12 \pm 0.32$	$1.32 \pm 0.06 \pm 0.29$	$1.51 \pm 0.06 \pm 0.27$	$1.40 \pm 0.06 \pm 0.29$	$1.31^{+0.20}_{-0.20}$
28–35	10^2	$4.88 \pm 0.42 \pm 0.87$	$5.09 \pm 0.25 \pm 0.82$	$5.03 \pm 0.26 \pm 0.77$	$5.33 \pm 0.25 \pm 0.91$	$4.70^{+0.65}_{-0.65}$
35–44.1	10^2	$1.73 \pm 0.17 \pm 0.26$	$1.79 \pm 0.09 \pm 0.23$	$1.89 \pm 0.10 \pm 0.25$	$1.92 \pm 0.09 \pm 0.27$	$1.66^{+0.22}_{-0.22}$
44.1–55.6	10^1	$6.21 \pm 0.64 \pm 0.72$	$6.01 \pm 0.40 \pm 0.69$	$6.60 \pm 0.44 \pm 0.83$	$6.42 \pm 0.40 \pm 0.96$	$5.66^{+0.85}_{-0.85}$
55.6–70	10^1	$2.07 \pm 0.33 \pm 0.25$	$2.12 \pm 0.19 \pm 0.24$	$1.97 \pm 0.19 \pm 0.23$	$2.16 \pm 0.21 \pm 0.34$	$1.88^{+0.22}_{-0.22}$
70–88.2	10^0	$8.06 \pm 1.39 \pm 0.83$	$6.96 \pm 1.11 \pm 0.83$	$7.43 \pm 0.81 \pm 0.90$	$6.66 \pm 0.81 \pm 0.98$	$6.05^{+0.84}_{-0.84}$
88.2–140	10^{-1}	$8.60 \pm 2.59 \pm 0.87$	$11.96 \pm 1.45 \pm 0.99$	$8.99 \pm 2.09 \pm 1.08$	$11.79 \pm 1.49 \pm 1.40$	$11.26^{+1.41}_{-1.39}$
140–280	10^{-2}		$5.16 \pm 1.62 \pm 0.41$	$6.47 \pm 2.29 \pm 0.65$	$5.63 \pm 1.42 \pm 0.58$	$5.32^{+0.77}_{-0.74}$

TABLE V. $\langle T_{AA} \rangle$-scaled prompt photon yields compared with JETPHOX 1.3 pp for $1.52 \leqslant |\eta| < 2.37$ in four centrality intervals and for JETPHOX as a function of photon p_T. For each value, the first uncertainty is statistical and the second is systematic. For JETPHOX, the combined error is shown.

| p_T (GeV) | Scale | $dN/dp_T / \langle T_{AA} \rangle$ (pb/GeV) | | | | $d\sigma/dp_T$ (pb/GeV) |
		40%–80%	20%–40%	10%–20%	0%–10%	JETPHOX
22–28	10^2	$6.82 \pm 1.11 \pm 1.70$	$7.08 \pm 0.56 \pm 1.49$	$6.52 \pm 0.66 \pm 1.74$	$7.22 \pm 0.55 \pm 1.82$	$7.90^{+1.33}_{-1.34}$
28–35	10^2	$2.22 \pm 0.44 \pm 0.53$	$2.50 \pm 0.24 \pm 0.50$	$2.38 \pm 0.28 \pm 0.61$	$2.36 \pm 0.24 \pm 0.61$	$2.80^{+0.45}_{-0.45}$
35–44.1	10^1	$7.13 \pm 1.95 \pm 1.60$	$8.13 \pm 1.14 \pm 1.64$	$9.32 \pm 0.98 \pm 1.87$	$7.48 \pm 1.39 \pm 1.53$	$9.62^{+1.35}_{-1.35}$
44.1–55.6	10^1	$2.34 \pm 0.85 \pm 0.54$	$3.10 \pm 0.41 \pm 0.50$	$3.62 \pm 0.26 \pm 0.50$	$3.13 \pm 0.28 \pm 0.49$	$3.13^{+0.52}_{-0.52}$
55.6–70	10^0	$8.78 \pm 1.87 \pm 1.20$	$9.08 \pm 2.16 \pm 1.40$	$11.86 \pm 1.24 \pm 1.63$	$6.41 \pm 2.25 \pm 0.88$	$9.56^{+1.69}_{-1.69}$
70–88.2	10^0	$2.13 \pm 0.72 \pm 0.32$	$2.04 \pm 0.54 \pm 0.27$	$2.98 \pm 0.52 \pm 0.37$	$2.19 \pm 0.54 \pm 0.42$	$2.68^{+0.45}_{-0.45}$
88.2–140	10^{-1}	$2.39 \pm 1.26 \pm 0.35$	$4.04 \pm 1.10 \pm 0.54$	$3.61 \pm 0.95 \pm 0.46$	$3.15 \pm 1.01 \pm 0.55$	$3.74^{+0.55}_{-0.55}$

TABLE VI. $\langle T_{AA} \rangle$-scaled prompt photon yields divided by the cross section from pp JETPHOX 1.3, for $|\eta| < 1.37$ in four centrality intervals as a function of photon p_T.

| p_T (GeV) | $dN/dp_T/\langle T_{AA} \rangle /d\sigma/dp_T$ (JETPHOX) | | | | |
	40%–80%	20%–40%	10%–20%	0%–10%	JETPHOX
22–28	$0.95 \pm 0.09 \pm 0.24$	$1.01 \pm 0.05 \pm 0.22$	$1.15 \pm 0.04 \pm 0.20$	$1.07 \pm 0.04 \pm 0.22$	$1^{+0.15}_{-0.15}$
28–35	$1.04 \pm 0.09 \pm 0.18$	$1.08 \pm 0.05 \pm 0.17$	$1.07 \pm 0.06 \pm 0.16$	$1.13 \pm 0.05 \pm 0.19$	$1^{+0.14}_{-0.14}$
35–44.1	$1.05 \pm 0.11 \pm 0.16$	$1.08 \pm 0.06 \pm 0.14$	$1.14 \pm 0.06 \pm 0.15$	$1.16 \pm 0.05 \pm 0.16$	$1^{+0.13}_{-0.13}$
44.1–55.6	$1.10 \pm 0.11 \pm 0.13$	$1.06 \pm 0.07 \pm 0.12$	$1.17 \pm 0.08 \pm 0.15$	$1.13 \pm 0.07 \pm 0.17$	$1^{+0.15}_{-0.15}$
55.6–70	$1.10 \pm 0.18 \pm 0.13$	$1.13 \pm 0.10 \pm 0.13$	$1.05 \pm 0.10 \pm 0.12$	$1.15 \pm 0.11 \pm 0.18$	$1^{+0.12}_{-0.12}$
70–88.2	$1.33 \pm 0.23 \pm 0.14$	$1.15 \pm 0.18 \pm 0.14$	$1.23 \pm 0.13 \pm 0.15$	$1.10 \pm 0.13 \pm 0.16$	$1^{+0.14}_{-0.14}$
88.2–140	$0.76 \pm 0.23 \pm 0.08$	$1.06 \pm 0.13 \pm 0.09$	$0.80 \pm 0.19 \pm 0.10$	$1.05 \pm 0.13 \pm 0.12$	$1^{+0.12}_{-0.12}$
140–280		$0.97 \pm 0.30 \pm 0.08$	$1.22 \pm 0.43 \pm 0.12$	$1.06 \pm 0.27 \pm 0.11$	$1^{+0.15}_{-0.14}$

TABLE VII. $\langle T_{AA} \rangle$-scaled prompt photon yields divided by the cross section from pp JETPHOX 1.3, for $1.52 \leqslant |\eta| < 2.37$ in four centrality intervals as a function of photon p_T.

| p_T (GeV) | $dN/dp_T/\langle T_{AA} \rangle /d\sigma/dp_T$ (JETPHOX) | | | | |
	40%–80%	20%–40%	10%–20%	0%–10%	JETPHOX
22–28	$0.86 \pm 0.14 \pm 0.22$	$0.90 \pm 0.07 \pm 0.19$	$0.83 \pm 0.08 \pm 0.22$	$0.91 \pm 0.07 \pm 0.23$	$1^{+0.17}_{-0.17}$
28–35	$0.79 \pm 0.16 \pm 0.19$	$0.89 \pm 0.09 \pm 0.18$	$0.85 \pm 0.10 \pm 0.22$	$0.84 \pm 0.09 \pm 0.22$	$1^{+0.16}_{-0.16}$
35–44.1	$0.74 \pm 0.20 \pm 0.17$	$0.84 \pm 0.12 \pm 0.17$	$0.97 \pm 0.10 \pm 0.19$	$0.78 \pm 0.14 \pm 0.16$	$1^{+0.14}_{-0.14}$
44.1–55.6	$0.75 \pm 0.27 \pm 0.17$	$0.99 \pm 0.13 \pm 0.16$	$1.16 \pm 0.08 \pm 0.16$	$1.00 \pm 0.09 \pm 0.15$	$1^{+0.17}_{-0.17}$
55.6–70	$0.92 \pm 0.20 \pm 0.13$	$0.95 \pm 0.23 \pm 0.15$	$1.24 \pm 0.13 \pm 0.17$	$0.67 \pm 0.24 \pm 0.09$	$1^{+0.18}_{-0.18}$
70–88.2	$0.80 \pm 0.27 \pm 0.12$	$0.76 \pm 0.20 \pm 0.10$	$1.11 \pm 0.19 \pm 0.14$	$0.82 \pm 0.20 \pm 0.16$	$1^{+0.17}_{-0.17}$
88.2–140	$0.64 \pm 0.34 \pm 0.09$	$1.08 \pm 0.29 \pm 0.15$	$0.97 \pm 0.26 \pm 0.12$	$0.84 \pm 0.27 \pm 0.15$	$1^{+0.15}_{-0.15}$
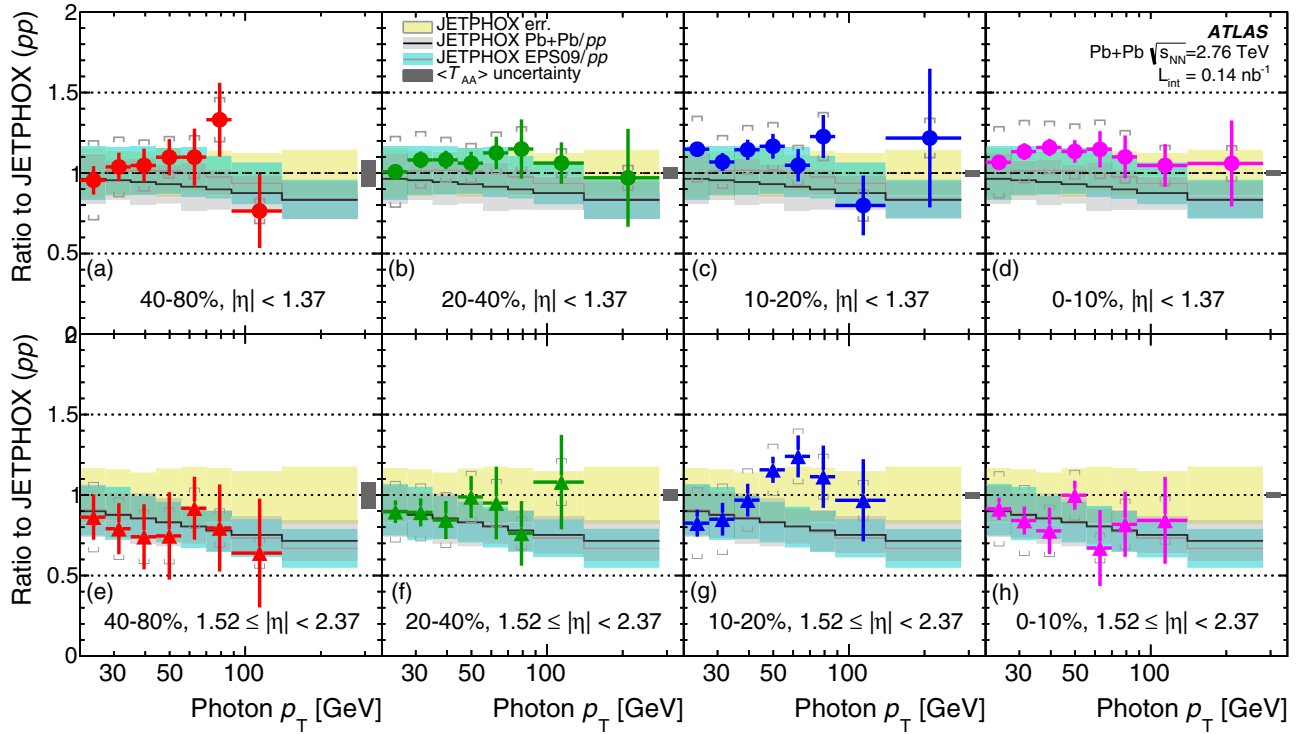
FIG. 7. Fully corrected normalized yields of prompt photons as a function of p_T in $|\eta| < 1.37$ [(a)–(d)] and $1.52 \leqslant |\eta| < 2.37$ [(e)–(h)] using tight photon selection, isolation cone size $\Delta R_{iso} = 0.3$, and isolation transverse energy of less than 6 GeV, divided by JETPHOX predictions for pp collisions, which implement the same isolation selection. The combined scale and PDF uncertainty on the JETPHOX calculation is shown by the gray line with yellow area. In addition, two other JETPHOX calculations are shown, also divided by the pp results: Pb + Pb collisions with no nuclear modification (black line with gray area) and Pb + Pb collisions with EPS09 nuclear modifications (gray line with blue area). Statistical uncertainties are shown by the bars. Systematic uncertainties on the photon yields are combined and shown by the upper and lower braces. The scale uncertainties owing only to $\langle T_{AA} \rangle$ are tabulated for each bin in Table I.

for Pb + Pb (both with $A = 208$) collisions using the standard PDF. The other incorporates nuclear modifications to the nucleon parton distributions using the EPS09 [1] PDF set, which are x- and Q^2-dependent modifications of the CTEQ 6.1

PDF, defined as ratios of the standard PDF as a function of x at a hardness scale $Q_0^2 = 1.69 \, \text{GeV}^2$ and evolved to the relevant Q^2 using standard DGLAP evolution. The EPS09 modifications have their own set of 15 uncertainty eigenvectors, which are
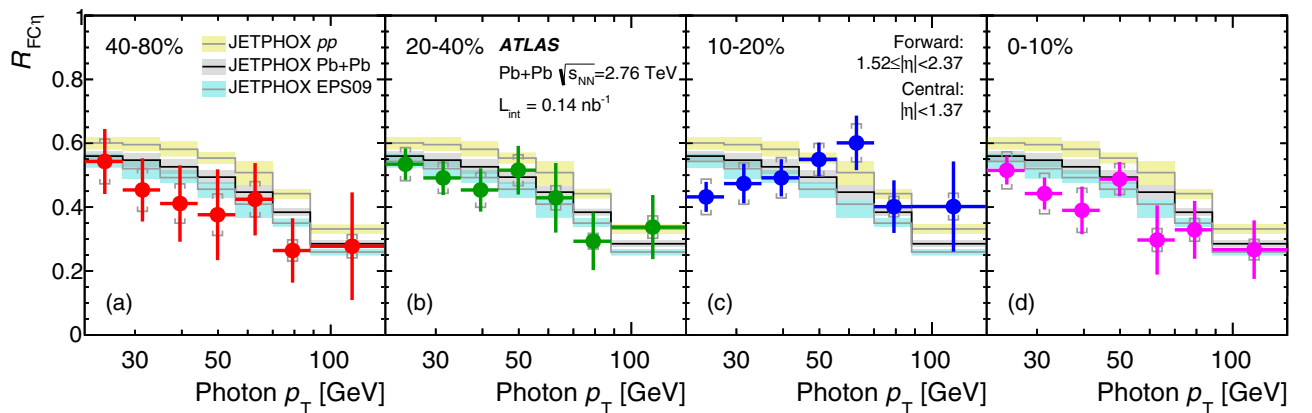

FIG. 8. Fully corrected yields of prompt photons as a function of p_T in $1.52 \leqslant |\eta| < 2.37$ divided by that measured in $|\eta| < 1.37$ using the tight photon selection, isolation cone size $\Delta R_{iso} = 0.3$, and isolation transverse energy of 6 GeV for four centrality intervals [(a)–(d)]. The yield ratio is compared to JETPHOX 1.3 predictions that implement the same isolation selection for three different configurations: pp collisions (gray line with yellow area), Pb + Pb collisions with no nuclear modification (black line with grey area), and Pb + Pb collisions with EPS09 nuclear modifications (gray line with blue area). Statistical uncertainties are shown by the bars. Systematic uncertainties on the photon yields are combined and shown by the braces.

TABLE VIII. Results for $R_{FC\eta}$, the prompt photon yield in the forward η region divided by that in the central η region, as a function of photon p_T for four centrality bins [(a)–(d)]. JETPHOX 1.3 pp calculations are also provided.

	$R_{FC\eta} = dN/dp_T(1.52 \leqslant |\eta| < 2.37)/dN/dp_T(|\eta| < 1.37)$				
p_T (GeV)	40%–80%	20%–40%	10%–20%	0%–10%	JETPHOX
22–28	$0.54 \pm 0.10 \pm 0.07$	$0.53 \pm 0.05 \pm 0.05$	$0.43 \pm 0.05 \pm 0.06$	$0.52 \pm 0.04 \pm 0.06$	$0.60^{+0.02}_{-0.02}$
28–35	$0.45 \pm 0.10 \pm 0.07$	$0.49 \pm 0.05 \pm 0.05$	$0.47 \pm 0.06 \pm 0.06$	$0.44 \pm 0.05 \pm 0.06$	$0.60^{+0.02}_{-0.02}$
35–44.1	$0.41 \pm 0.12 \pm 0.06$	$0.45 \pm 0.07 \pm 0.05$	$0.49 \pm 0.06 \pm 0.06$	$0.39 \pm 0.07 \pm 0.07$	$0.58^{+0.03}_{-0.02}$
44.1–55.6	$0.38 \pm 0.14 \pm 0.06$	$0.52 \pm 0.08 \pm 0.05$	$0.55 \pm 0.05 \pm 0.05$	$0.49 \pm 0.05 \pm 0.05$	$0.55^{+0.02}_{-0.02}$
55.6–70	$0.42 \pm 0.11 \pm 0.06$	$0.43 \pm 0.11 \pm 0.04$	$0.60 \pm 0.09 \pm 0.06$	$0.30 \pm 0.11 \pm 0.04$	$0.51^{+0.04}_{-0.04}$
70–88.2	$0.26 \pm 0.10 \pm 0.03$	$0.29 \pm 0.09 \pm 0.02$	$0.40 \pm 0.08 \pm 0.03$	$0.33 \pm 0.09 \pm 0.04$	$0.44^{+0.02}_{-0.02}$
88.2–140	$0.28 \pm 0.17 \pm 0.04$	$0.34 \pm 0.10 \pm 0.03$	$0.40 \pm 0.14 \pm 0.04$	$0.27 \pm 0.09 \pm 0.03$	$0.33^{+0.01}_{-0.02}$

used to evaluate 30 variations of the cross sections relative to the default set, which are typically approximately 5%, with only a small variation in p_T.

IX. RESULTS

The per-event differential photon yields are calculated according to Eq. (2). These are then divided by $\langle T_{AA} \rangle$ for comparison with the JETPHOX calculations. The results are shown as a function of p_T in Fig. 6 and are tabulated in Table IV for $|\eta| < 1.37$ and in Table V for $1.52 \leqslant |\eta| < 2.37$. Each panel shows a single pseudorapidity interval, with four centrality intervals, each scaled by a factor of 10 relative to each other.

The ratios of the data to the JETPHOX pp predictions are shown in Fig. 7 and are tabulated in Table VI for $|\eta| < 1.37$ and in Table VII for $1.52 \leqslant |\eta| < 2.37$. In addition, the two other JETPHOX calculations described in the previous section are shown, also divided by the pp results: Pb + Pb collisions with no nuclear modification (black line) and Pb + Pb collisions with EPS09 nuclear modifications (hatched blue area). The combined scale and PDF uncertainty on the JETPHOX calculations, calculated separately for each configuration, are shown as shaded regions. The data are found to agree well with the JETPHOX pp prediction in all centrality and η regions, within the stated statistical and systematic uncertainties. They are also consistent within uncertainties of the other physics scenarios as well. Thus, the current data are not of sufficient precision to address nuclear PDF effects quantitatively. However, it should be noted that where the data are more precise, in the central η region, the PDF modifications implemented in EPS09 compensate for the suppression at higher p_T seen in the Pb + Pb calculations, giving cross sections similar to the pp case.

The ratios $R_{FC\eta}$ of cross sections between the forward and central η intervals are calculated as a function of p_T for each centrality interval and are shown in Fig. 8, as well as tabulated in Table VIII. Evaluation of these ratios leads to the cancellation of several systematic effects on the efficiencies and bin-by-bin correction factors, mitigate the effect of the theoretical uncertainties, and fully remove the uncertainty on $\langle T_{AA} \rangle$. The results are compared to JETPHOX

calculations for pp (yellow region), Pb + Pb (black line with gray area), and EPS09 nPDF (gray line with blue area). It is clear that there is some sensitivity to the nuclear PDF, primarily through the expected depletion of photon yields in the forward direction expected when including the neutron PDF to match the isospin composition of the lead nuclei. While the data are consistent with all three curves within the statistical and systematic uncertainties, a slight preference for the calculations incorporating isospin effects is observed.

X. CONCLUSIONS

In this paper, measured yields of isolated prompt photons in 0.14 nb^{-1} lead-lead collisions recorded by the ATLAS detector at the LHC have been presented as a function of collision centrality (in four intervals from 40%–80% to 0%–10%) in two pseudorapidity regions ($|\eta| < 1.37$ and $1.52 \leqslant |\eta| < 2.37$) and for photon transverse momenta in the range $22 \leqslant p_T < 280$ GeV. Photons were reconstructed using the large-acceptance, longitudinally segmented electromagnetic calorimeter, after an event-by-event subtraction of the average underlying event in each calorimeter layer in small $\Delta\eta$ intervals. Backgrounds stemming from neutral hadrons in jets are suppressed by a tight shower shape selection and by requiring no more than 6 GeV transverse energy in a cone of size $\Delta R = 0.3$ around each photon. The residual hadronic background is determined using a double-sideband method, and the remaining signal is corrected for efficiency and resolution, as well as electron contamination, to arrive at the per-event yield of photons as a function of p_T in each η and centrality interval. After scaling the yields by the mean nuclear thickness $\langle T_{AA} \rangle$, the p_T spectrum in each η and centrality interval is found to agree, within statistical and systematic uncertainties, with next-to-leading-order perturbative QCD calculations of proton-proton collisions. The data are also compared with calculations that assume the isospin of Pb + Pb collisions, as well as the calculations for Pb + Pb using the EPS09 nuclear modifications of the proton parton distribution functions. The ratios of the forward yields to those near midrapidity ($R_{FC\eta}$) are also shown, and are compared to the corresponding ratios from JETPHOX. The present data are

unable to distinguish between the three scenarios. However, the overall consistency of the measured yields with JETPHOX expectations for all centrality intervals demonstrates that photon yields in heavy-ion collisions scale as expected with the mean nuclear thickness. This provides further support for the interpretation of the clear modification of jet yields in Pb + Pb collisions as a function of centrality, relative to those measured in proton-proton collisions, as stemming from energy loss in the hot, dense medium [52].

[1] K. Eskola, H. Paukkunen, and C. Salgado, J. High Energy Phys. 04 (2009) 065.

[2] M. Hirai, S. Kumano, and T.-H. Nagai, Phys. Rev. C **76**, 065207 (2007).

[3] D. de Florian and R. Sassot, Phys. Rev. D **69**, 074028 (2004).

[4] J. Aubert *et al.*, Phys. Lett. B **123**, 275 (1983).

[5] R. J. Fries, B. Muller, and D. K. Srivastava, Phys. Rev. Lett. **90**, 132301 (2003).

[6] S. Turbide, C. Gale, S. Jeon, and G. D. Moore, Phys. Rev. C **72**, 014906 (2005).

[7] S. Catani *et al.*, J. High Energy Phys. 05 (2002) 028.

[8] M. Bonesini *et al.* (WA70 Collaboration), Z. Phys. C **37**, 535 (1988).

[9] G. Ballocchi *et al.* (UA6 Collaboration), Phys. Lett. B **436**, 222 (1998).

[10] L. Apanasevich *et al.* (E706 Collaboration), Phys. Rev. D **70**, 092009 (2004).

[11] E. Anassontzis *et al.*, Z. Phys. C **13**, 277 (1982).

[12] A. Angelis *et al.* (CMOR Collaboration), Nucl. Phys. B **327**, 541 (1989).

[13] A. Adare *et al.* (PHENIX Collaboration), Phys. Rev. D **86**, 072008 (2012).

[14] B. Abelev *et al.* (STAR Collaboration), Phys. Rev. C **81**, 064904 (2010).

[15] C. Albajar *et al.* (UA1 Collaboration), Phys. Lett. B **209**, 385 (1988).

[16] J. Alitti *et al.* (UA2 Collaboration), Phys. Lett. B **288**, 386 (1992).

[17] B. Abbott *et al.* (D0 Collaboration), Phys. Rev. Lett. **84**, 2786 (2000).

[18] D. Acosta *et al.* (CDF Collaboration), Phys. Rev. D **65**, 112003 (2002).

[19] V. Abazov *et al.* (D0 Collaboration), Phys. Lett. B **639**, 151 (2006).

[20] T. Aaltonen *et al.* (CDF Collaboration), Phys. Rev. D **80**, 111106 (2009).

[21] ATLAS Collaboration, Phys. Rev. D **83**, 052005 (2011).

[22] ATLAS Collaboration, Phys. Lett. B **706**, 150 (2011).

[23] ATLAS Collaboration, Phys. Rev. D **89**, 052004 (2014).

[24] CMS Collaboration, Phys. Rev. Lett. **106**, 082001 (2011).

[25] CMS Collaboration, Phys. Rev. D **84**, 052011 (2011).

[26] P. Aurenche, J. P. Guillet, E. Pilon, M. Werlen, and M. Fontannaz, Phys. Rev. D **73**, 094007 (2006).

[27] M. Aggarwal *et al.* (WA98 Collaboration), Phys. Rev. Lett. **85**, 3595 (2000).

[28] S. Adler *et al.* (PHENIX Collaboration), Phys. Rev. Lett. **94**, 232301 (2005).

[29] S. Afanasiev *et al.* (PHENIX Collaboration), Phys. Rev. Lett. **109**, 152302 (2012).

[30] CMS Collaboration, Phys. Lett. B **710**, 256 (2012).

[31] ATLAS Collaboration, J. Instrum. **3**, S08003 (2008).

[32] ATLAS Collaboration, ATLAS-CONF-2010-005 (2010), https://cds.cern.ch/record/1273197.

[33] M. L. Miller *et al.*, Annu. Rev. Nucl. Part. Sci. **57**, 205 (2007).

[34] R. Achenbach *et al.*, J. Instrum. **3**, P03001 (2008).

[35] ATLAS Collaboration, Phys. Lett. B **707**, 330 (2012).

[36] ATLAS Collaboration, Phys. Lett. B **710**, 363 (2012).

[37] T. Sjostrand, S. Mrenna, and P. Z. Skands, J. High Energy Phys. 05 (2006) 026.

[38] ATLAS Collaboration, ATLAS-PHYS-PUB-2011-009 (2011), http://cdsweb.cern.ch/record/1363300.

[39] T. Gleisberg *et al.*, J. High Energy Phys. 02 (2009) 007.

[40] H.-L. Lai, M. Guzzi, J. Huston, Z. Li, P. M. Nadolsky, J. Pumplin, and C.-P. Yuan, Phys. Rev. D **82**, 074024 (2010).

[41] S. Agostinelli *et al.* (GEANT4 Collaboration), Nucl. Instrum. Methods A **506**, 250 (2003).

[42] ATLAS Collaboration, Eur. Phys. J. C **70**, 823 (2010).

[43] ATLAS Collaboration, ATL-PHYS-PUB-2011-007 (2011), https://cds.cern.ch/record/1345329.

[44] ATLAS Collaboration, Phys. Lett. B **719**, 220 (2013).

[45] A. M. Poskanzer and S. A. Voloshin, Phys. Rev. C **58**, 1671 (1998).

[46] ATLAS Collaboration, Eur. Phys. J. C **72**, 1909 (2012).

[47] S. Frixione, P. Nason, and C. Oleari, J. High Energy Phys. 11 (2007) 070.

[48] T. Sjostrand, S. Mrenna, and P. Z. Skands, Comput. Phys. Commun. **178**, 852 (2008).

[49] P. M. Nadolsky, H. L. Lai, Q. H. Cao, J. Huston, J. Pumplin, D. Stump, W. K. Tung, and C. P. Yuan, Phys. Rev. D **78**, 013004 (2008).

[50] L. Bourhis, M. Fontannaz, and J. Guillet, Eur. Phys. J. C **2**, 529 (1998).

[51] A. Martin *et al.*, Eur. Phys. J. C **63**, 189 (2009).

[52] ATLAS Collaboration, Phys. Rev. Lett. **114**, 072302 (2015).

G. Aad,[84] B. Abbott,[112] J. Abdallah,[152] S. Abdel Khalek,[116] O. Abdinov,[11] R. Aben,[106] B. Abi,[113] M. Abolins,[89] O. S. AbouZeid,[159] H. Abramowicz,[154] H. Abreu,[153] R. Abreu,[30] Y. Abulaiti,[147a,147b] B. S. Acharya,[165a,165b,a] L. Adamczyk,[38a] D. L. Adams,[25] J. Adelman,[177] S. Adomeit,[99] T. Adye,[130] T. Agatonovic-Jovin,[13] J. A. Aguilar-Saavedra,[125a,125f] M. Agustoni,[17] S. P. Ahlen,[22] F. Ahmadov,[64,b] G. Aielli,[134a,134b] H. Akerstedt,[147a,147b] T. P. A. Åkesson,[80] G. Akimoto,[156] A. V. Akimov,[95] G. L. Alberghi,[20a,20b] J. Albert,[170] S. Albrand,[55] M. J. Alconada Verzini,[70] M. Aleksa,[30] I. N. Aleksandrov,[64] C. Alexa,[26a] G. Alexander,[154] G. Alexandre,[49] T. Alexopoulos,[10] M. Alhroob,[165a,165c] G. Alimonti,[90a] L. Alio,[84] J. Alison,[31] B. M. M. Allbrooke,[18] L. J. Allison,[71] P. P. Allport,[73] J. Almond,[83] A. Aloisio,[103a,103b] A. Alonso,[36] F. Alonso,[70] C. Alpigiani,[75] A. Altheimer,[35] B. Alvarez Gonzalez,[89] M. G. Alviggi,[103a,103b] K. Amako,[65] Y. Amaral Coutinho,[24a] C. Amelung,[23] D. Amidei,[88] S. P. Amor Dos Santos,[125a,125c] A. Amorim,[125a,125b] S. Amoroso,[48] N. Amram,[154] G. Amundsen,[23] C. Anastopoulos,[140] L. S. Ancu,[49] N. Andari,[30] T. Andeen,[35] C. F. Anders,[58b] G. Anders,[30] K. J. Anderson,[31] A. Andreazza,[90a,90b] V. Andrei,[58a] X. S. Anduaga,[70] S. Angelidakis,[9] I. Angelozzi,[106] P. Anger,[44] A. Angerami,[35] F. Anghinolfi,[30] A. V. Anisenkov,[108,c] N. Anjos,[125a] A. Annovi,[47] A. Antonaki,[9] M. Antonelli,[47] A. Antonov,[97] J. Antos,[145b] F. Anulli,[133a] M. Aoki,[65] L. Aperio Bella,[18] R. Apolle,[119,d] G. Arabidze,[89] I. Aracena,[144] Y. Arai,[65] J. P. Araque,[125a] A. T. H. Arce,[45] J-F. Arguin,[94] S. Argyropoulos,[42] M. Arik,[19a] A. J. Armbruster,[30] O. Arnaez,[30] V. Arnal,[81] H. Arnold,[48] M. Arratia,[28] O. Arslan,[21] A. Artamonov,[96] G. Artoni,[23] S. Asai,[156] N. Asbah,[42] A. Ashkenazi,[154] B. Åsman,[147a,147b] L. Asquith,[6] K. Assamagan,[25] R. Astalos,[145a] M. Atkinson,[166] N. B. Atlay,[142] B. Auerbach,[6] K. Augsten,[127] M. Aurousseau,[146b] G. Avolio,[30] G. Azuelos,[94,e] Y. Azuma,[156] M. A. Baak,[30] A. E. Baas,[58a] C. Bacci,[135a,135b] H. Bachacou,[137] K. Bachas,[155] M. Backes,[30] M. Backhaus,[30] J. Backus Mayes,[144] E. Badescu,[26a] P. Bagiacchi,[133a,133b] P. Bagnaia,[133a,133b] Y. Bai,[33a] T. Bain,[35] J. T. Baines,[130] O. K. Baker,[177] P. Balek,[128] F. Balli,[137] E. Banas,[39] Sw. Banerjee,[174] A. A. E. Bannoura,[176] V. Bansal,[170] H. S. Bansil,[18] L. Barak,[173] E. L. Barberio,[87] D. Barberis,[50a,50b] M. Barbero,[84] T. Barillari,[100] M. Barisonzi,[176] T. Barklow,[144] N. Barlow,[28] B. M. Barnett,[130] R. M. Barnett,[15] Z. Barnovska,[5] A. Baroncelli,[135a] G. Barone,[49] A. J. Barr,[119] F. Barreiro,[81] J. Barreiro Guimarães da Costa,[57] R. Bartoldus,[144] A. E. Barton,[71] P. Bartos,[145a] V. Bartsch,[150] A. Bassalat,[116] A. Basye,[166] R. L. Bates,[53] J. R. Batley,[28] M. Battaglia,[138] M. Battistin,[30] F. Bauer,[137] H. S. Bawa,[144,f] M. D. Beattie,[71] T. Beau,[79] P. H. Beauchemin,[162] R. Beccherle,[123a,123b] P. Bechtle,[21] H. P. Beck,[17,g] K. Becker,[176] S. Becker,[99] M. Beckingham,[171] C. Becot,[116] A. J. Beddall,[19c] A. Beddall,[19c] S. Bedikian,[177] V. A. Bednyakov,[64] C. P. Bee,[149] L. J. Beemster,[106] T. A. Beermann,[176] M. Begel,[25] J. K. Behr,[119] C. Belanger-Champagne,[86] P. J. Bell,[49] W. H. Bell,[49] G. Bella,[154] L. Bellagamba,[20a] A. Bellerive,[29] M. Bellomo,[85] K. Belotskiy,[97] O. Beltramello,[30] O. Benary,[154] D. Benchekroun,[136a] K. Bendtz,[147a,147b] N. Benekos,[166] Y. Benhammou,[154] E. Benhar Noccioli,[49] J. A. Benitez Garcia,[160b] D. P. Benjamin,[45] J. R. Bensinger,[23] K. Benslama,[131] S. Bentvelsen,[106] D. Berge,[106] E. Bergeaas Kuutmann,[167] N. Berger,[5] F. Berghaus,[170] J. Beringer,[15] C. Bernard,[22] P. Bernat,[77] C. Bernius,[78] F. U. Bernlochner,[170] T. Berry,[76] P. Berta,[128] C. Bertella,[84] G. Bertoli,[147a,147b] F. Bertolucci,[123a,123b] C. Bertsche,[112] D. Bertsche,[112] M. I. Besana,[90a] G. J. Besjes,[105] O. Bessidskaia Bylund,[147a,147b] M. Bessner,[42] N. Besson,[137] C. Betancourt,[48] S. Bethke,[100] W. Bhimji,[46] R. M. Bianchi,[124] L. Bianchini,[23] M. Bianco,[30] O. Biebel,[99] S. P. Bieniek,[77] K. Bierwagen,[54] J. Biesiada,[15] M. Biglietti,[135a] J. Bilbao De Mendizabal,[49] H. Bilokon,[47] M. Bindi,[54] S. Binet,[116] A. Bingul,[19c] C. Bini,[133a,133b] C. W. Black,[151] J. E. Black,[144] K. M. Black,[22] D. Blackburn,[139] R. E. Blair,[6] J.-B. Blanchard,[137] T. Blazek,[145a] I. Bloch,[42] C. Blocker,[23] W. Blum,[82,*] U. Blumenschein,[54] G. J. Bobbink,[106] V. S. Bobrovnikov,[108,c] S. S. Bocchetta,[80] A. Bocci,[45] C. Bock,[99] C. R. Boddy,[119] M. Boehler,[48] T. T. Boek,[176] J. A. Bogaerts,[30] A. G. Bogdanchikov,[108] A. Bogouch,[91,*] C. Bohm,[147a] J. Bohm,[126] V. Boisvert,[76] T. Bold,[38a] V. Boldea,[26a] A. S. Boldyrev,[98] M. Bomben,[79] M. Bona,[75] M. Boonekamp,[137] A. Borisov,[129] G. Borissov,[71] M. Borri,[83] S. Borroni,[42] J. Bortfeldt,[99] V. Bortolotto,[135a,135b] K. Bos,[106] D. Boscherini,[20a] M. Bosman,[12] H. Boterenbrood,[106] J. Boudreau,[124] J. Bouffard,[2] E. V. Bouhova-Thacker,[71] D. Boumediene,[34] C. Bourdarios,[116] N. Bousson,[113] S. Boutouil,[136d] A. Boveia,[31] J. Boyd,[30] I. R. Boyko,[64] J. Bracinik,[18] A. Brandt,[8] G. Brandt,[15] O. Brandt,[58a] U. Bratzler,[157] B. Brau,[85] J. E. Brau,[115] H. M. Braun,[176,*] S. F. Brazzale,[165a,165c] B. Brelier,[159] K. Brendlinger,[121] A. J. Brennan,[87] R. Brenner,[167]

S. Bressler,[173] K. Bristow,[146c] T. M. Bristow,[46] D. Britton,[53] F. M. Brochu,[28] I. Brock,[21] R. Brock,[89] C. Bromberg,[89] J. Bronner,[100] G. Brooijmans,[35] T. Brooks,[76] W. K. Brooks,[32b] J. Brosamer,[15] E. Brost,[115] J. Brown,[55] P. A. Bruckman de Renstrom,[39] D. Bruncko,[145b] R. Bruneliere,[48] S. Brunet,[60] A. Bruni,[20a] G. Bruni,[20a] M. Bruschi,[20a] L. Bryngemark,[80] T. Buanes,[14] Q. Buat,[143] F. Bucci,[49] P. Buchholz,[142] R. M. Buckingham,[119] A. G. Buckley,[53] S. I. Buda,[26a] I. A. Budagov,[64] F. Buehrer,[48] L. Bugge,[118] M. K. Bugge,[118] O. Bulekov,[97] A. C. Bundock,[73] H. Burckhart,[30] S. Burdin,[73] B. Burghgrave,[107] S. Burke,[130] I. Burmeister,[43] E. Busato,[34] D. Büscher,[48] V. Büscher,[82] P. Bussey,[53] C. P. Buszello,[167] B. Butler,[57] J. M. Butler,[22] A. I. Butt,[3] C. M. Buttar,[53] J. M. Butterworth,[77] P. Butti,[106] W. Buttinger,[28] A. Buzatu,[53] M. Byszewski,[10] S. Cabrera Urbán,[168] D. Caforio,[20a,20b] O. Cakir,[4a] P. Calafiura,[15] A. Calandri,[137] G. Calderini,[79] P. Calfayan,[99] R. Calkins,[107] L. P. Caloba,[24a] D. Calvet,[34] S. Calvet,[34] R. Camacho Toro,[49] S. Camarda,[42] D. Cameron,[118] L. M. Caminada,[15] R. Caminal Armadans,[12] S. Campana,[30] M. Campanelli,[77] A. Campoverde,[149] V. Canale,[103a,103b] A. Canepa,[160a] M. Cano Bret,[75] J. Cantero,[81] R. Cantrill,[125a] T. Cao,[40] M. D. M. Capeans Garrido,[30] I. Caprini,[26a] M. Caprini,[26a] M. Capua,[37a,37b] R. Caputo,[82] R. Cardarelli,[134a] T. Carli,[30] G. Carlino,[103a] L. Carminati,[90a,90b] S. Caron,[105] E. Carquin,[32a] G. D. Carrillo-Montoya,[146c] J. R. Carter,[28] J. Carvalho,[125a,125c] D. Casadei,[77] M. P. Casado,[12] M. Casolino,[12] E. Castaneda-Miranda,[146b] A. Castelli,[106] V. Castillo Gimenez,[168] N. F. Castro,[125a,h] P. Catastini,[57] A. Catinaccio,[30] J. R. Catmore,[118] A. Cattai,[30] G. Cattani,[134a,134b] J. Caudron,[82] S. Caughron,[89] V. Cavaliere,[166] D. Cavalli,[90a] M. Cavalli-Sforza,[12] V. Cavasinni,[123a,123b] F. Ceradini,[135a,135b] B. C. Cerio,[45] K. Cerny,[128] A. S. Cerqueira,[24b] A. Cerri,[150] L. Cerrito,[75] F. Cerutti,[15] M. Cerv,[30] A. Cervelli,[17] S. A. Cetin,[19b] A. Chafaq,[136a] D. Chakraborty,[107] I. Chalupkova,[128] P. Chang,[166] B. Chapleau,[86] J. D. Chapman,[28] D. Charfeddine,[116] D. G. Charlton,[18] C. C. Chau,[159] C. A. Chavez Barajas,[150] S. Cheatham,[86] A. Chegwidden,[89] S. Chekanov,[6] S. V. Chekulaev,[160a] G. A. Chelkov,[64,i] M. A. Chelstowska,[88] C. Chen,[63] H. Chen,[25] K. Chen,[149] L. Chen,[33d,j] S. Chen,[33c] X. Chen,[146c] Y. Chen,[66] Y. Chen,[35] H. C. Cheng,[88] Y. Cheng,[31] A. Cheplakov,[64] R. Cherkaoui El Moursli,[136e] V. Chernyatin,[25,*] E. Cheu,[7] L. Chevalier,[137] V. Chiarella,[47] G. Chiefari,[103a,103b] J. T. Childers,[6] A. Chilingarov,[71] G. Chiodini,[72a] A. S. Chisholm,[18] R. T. Chislett,[77] A. Chitan,[26a] M. V. Chizhov,[64] S. Chouridou,[9] B. K. B. Chow,[99] D. Chromek-Burckhart,[30] M. L. Chu,[152] J. Chudoba,[126] J. J. Chwastowski,[39] L. Chytka,[114] G. Ciapetti,[133a,133b] A. K. Ciftci,[4a] R. Ciftci,[4a] D. Cinca,[53] V. Cindro,[74] A. Ciocio,[15] P. Cirkovic,[13] Z. H. Citron,[173] M. Ciubancan,[26a] A. Clark,[49] P. J. Clark,[46] R. N. Clarke,[15] W. Cleland,[124] J. C. Clemens,[84] C. Clement,[147a,147b] Y. Coadou,[84] M. Cobal,[165a,165c] A. Coccaro,[139] J. Cochran,[63] L. Coffey,[23] J. G. Cogan,[144] J. Coggeshall,[166] B. Cole,[35] S. Cole,[107] A. P. Colijn,[106] J. Collot,[55] T. Colombo,[58c] G. Colon,[85] G. Compostella,[100] P. Conde Muiño,[125a,125b] E. Coniavitis,[48] M. C. Conidi,[12] S. H. Connell,[146b] I. A. Connelly,[76] S. M. Consonni,[90a,90b] V. Consorti,[48] S. Constantinescu,[26a] C. Conta,[120a,120b] G. Conti,[57] F. Conventi,[103a,k] M. Cooke,[15] B. D. Cooper,[77] A. M. Cooper-Sarkar,[119] N. J. Cooper-Smith,[76] K. Copic,[15] T. Cornelissen,[176] M. Corradi,[20a] F. Corriveau,[86,l] A. Corso-Radu,[164] A. Cortes-Gonzalez,[12] G. Cortiana,[100] G. Costa,[90a] M. J. Costa,[168] D. Costanzo,[140] D. Côté,[8] G. Cottin,[28] G. Cowan,[76] B. E. Cox,[83] K. Cranmer,[109] G. Cree,[29] S. Crépé-Renaudin,[55] F. Crescioli,[79] W. A. Cribbs,[147a,147b] M. Crispin Ortuzar,[119] M. Cristinziani,[21] V. Croft,[105] G. Crosetti,[37a,37b] C.-M. Cuciuc,[26a] T. Cuhadar Donszelmann,[140] J. Cummings,[177] M. Curatolo,[47] C. Cuthbert,[151] H. Czirr,[142] P. Czodrowski,[3] Z. Czyczula,[177] S. D'Auria,[53] M. D'Onofrio,[73] M. J. Da Cunha Sargedas De Sousa,[125a,125b] C. Da Via,[83] W. Dabrowski,[38a] A. Dafinca,[119] T. Dai,[88] O. Dale,[14] F. Dallaire,[94] C. Dallapiccola,[85] M. Dam,[36] A. C. Daniells,[18] M. Dano Hoffmann,[137] V. Dao,[48] G. Darbo,[50a] S. Darmora,[8] J. Dassoulas,[42] A. Dattagupta,[60] W. Davey,[21] C. David,[170] T. Davidek,[128] E. Davies,[119,d] M. Davies,[154] O. Davignon,[79] A. R. Davison,[77] P. Davison,[77] Y. Davygora,[58a] E. Dawe,[143] I. Dawson,[140] R. K. Daya-Ishmukhametova,[85] K. De,[8] R. de Asmundis,[103a] S. De Castro,[20a,20b] S. De Cecco,[79] N. De Groot,[105] P. de Jong,[106] H. De la Torre,[81] F. De Lorenzi,[63] L. De Nooij,[106] D. De Pedis,[133a] A. De Salvo,[133a] U. De Sanctis,[165a,165b] A. De Santo,[150] J. B. De Vivie De Regie,[116] W. J. Dearnaley,[71] R. Debbe,[25] C. Debenedetti,[138] B. Dechenaux,[55] D. V. Dedovich,[64] I. Deigaard,[106] J. Del Peso,[81] T. Del Prete,[123a,123b] F. Deliot,[137] C. M. Delitzsch,[49] M. Deliyergiyev,[74] A. Dell'Acqua,[30] L. Dell'Asta,[22] M. Dell'Orso,[123a,123b] M. Della Pietra,[103a,k] D. della Volpe,[49] M. Delmastro,[5] P. A. Delsart,[55] C. Deluca,[106] S. Demers,[177] M. Demichev,[64] A. Demilly,[79] S. P. Denisov,[129] D. Derendarz,[39] J. E. Derkaoui,[136d] F. Derue,[79] P. Dervan,[73] K. Desch,[21] C. Deterre,[42] P. O. Deviveiros,[106] A. Dewhurst,[130] S. Dhaliwal,[106] A. Di Ciaccio,[134a,134b] L. Di Ciaccio,[5] A. Di Domenico,[133a,133b] C. Di Donato,[103a,103b] A. Di Girolamo,[30] B. Di Girolamo,[30] A. Di Mattia,[153] B. Di Micco,[135a,135b] R. Di Nardo,[47] A. Di Simone,[48] R. Di Sipio,[20a,20b] D. Di Valentino,[29] F. A. Dias,[46] M. A. Diaz,[32a] E. B. Diehl,[88] J. Dietrich,[42] T. A. Dietzsch,[58a] S. Diglio,[84] A. Dimitrievska,[13] J. Dingfelder,[21] C. Dionisi,[133a,133b] P. Dita,[26a] S. Dita,[26a] F. Dittus,[30] F. Djama,[84] T. Djobava,[51b] J. I. Djuvsland,[58a] M. A. B. do Vale,[24c] A. Do Valle Wemans,[125a,125g] T. K. O. Doan,[5] D. Dobos,[30] C. Doglioni,[49] T. Doherty,[53] T. Dohmae,[156] J. Dolejsi,[128] Z. Dolezal,[128] B. A. Dolgoshein,[97,*] M. Donadelli,[24d] S. Donati,[123a,123b] P. Dondero,[120a,120b] J. Donini,[34] J. Dopke,[130] A. Doria,[103a] M. T. Dova,[70] A. T. Doyle,[53] M. Dris,[10] J. Dubbert,[88] S. Dube,[15] E. Dubreuil,[34] E. Duchovni,[173] G. Duckeck,[99] O. A. Ducu,[26a] D. Duda,[176] A. Dudarev,[30] F. Dudziak,[63] L. Duflot,[116] L. Duguid,[76] M. Dührssen,[30] M. Dunford,[58a] H. Duran Yildiz,[4a] M. Düren,[52] A. Durglishvili,[51b] M. Dwuznik,[38a] M. Dyndal,[38a] J. Ebke,[99] W. Edson,[2] N. C. Edwards,[46] W. Ehrenfeld,[21] T. Eifert,[144] G. Eigen,[14] K. Einsweiler,[15] T. Ekelof,[167] M. El Kacimi,[136c] M. Ellert,[167] S. Elles,[5] F. Ellinghaus,[82] N. Ellis,[30] J. Elmsheuser,[99] M. Elsing,[30] D. Emeliyanov,[130] Y. Enari,[156] O. C. Endner,[82] M. Endo,[117] J. Erdmann,[177] A. Ereditato,[17] D. Eriksson,[147a] G. Ernis,[176] J. Ernst,[2] M. Ernst,[25] J. Ernwein,[137] D. Errede,[166] S. Errede,[166] E. Ertel,[82] M. Escalier,[116] H. Esch,[43] C. Escobar,[124] B. Esposito,[47] A. I. Etienvre,[137] E. Etzion,[154] H. Evans,[60] A. Ezhilov,[122] L. Fabbri,[20a,20b] G. Facini,[31] R. M. Fakhrutdinov,[129] S. Falciano,[133a] R. J. Falla,[77] J. Faltova,[128] Y. Fang,[33a] M. Fanti,[90a,90b] A. Farbin,[8] A. Farilla,[135a] T. Farooque,[12] S. Farrell,[15] S. M. Farrington,[171] P. Farthouat,[30] F. Fassi,[136e] P. Fassnacht,[30]

D. Fassouliotis,[9] A. Favareto,[50a,50b] L. Fayard,[116] P. Federic,[145a] O. L. Fedin,[122,m] W. Fedorko,[169] M. Fehling-Kaschek,[48] S. Feigl,[30] L. Feligioni,[84] C. Feng,[33d] E. J. Feng,[6] H. Feng,[88] A. B. Fenyuk,[129] S. Fernandez Perez,[30] S. Ferrag,[53] J. Ferrando,[53] A. Ferrari,[167] P. Ferrari,[106] R. Ferrari,[120a] D. E. Ferreira de Lima,[53] A. Ferrer,[168] D. Ferrere,[49] C. Ferretti,[88] A. Ferretto Parodi,[50a,50b] M. Fiascaris,[31] F. Fiedler,[82] A. Filipčič,[74] M. Filipuzzi,[42] F. Filthaut,[105] M. Fincke-Keeler,[170] K. D. Finelli,[151] M. C. N. Fiolhais,[125a,125c] L. Fiorini,[168] A. Firan,[40] A. Fischer,[2] J. Fischer,[176] W. C. Fisher,[89] E. A. Fitzgerald,[23] M. Flechl,[48] I. Fleck,[142] P. Fleischmann,[88] S. Fleischmann,[176] G. T. Fletcher,[140] G. Fletcher,[75] T. Flick,[176] A. Floderus,[80] L. R. Flores Castillo,[174,n] A. C. Florez Bustos,[160b] M. J. Flowerdew,[100] A. Formica,[137] A. Forti,[83] D. Fortin,[160a] D. Fournier,[116] H. Fox,[71] S. Fracchia,[12] P. Francavilla,[79] M. Franchini,[20a,20b] S. Franchino,[30] D. Francis,[30] L. Franconi,[118] M. Franklin,[57] S. Franz,[61] M. Fraternali,[120a,120b] S. T. French,[28] C. Friedrich,[42] F. Friedrich,[44] D. Froidevaux,[30] J. A. Frost,[28] C. Fukunaga,[157] E. Fullana Torregrosa,[82] B. G. Fulsom,[144] J. Fuster,[168] C. Gabaldon,[55] O. Gabizon,[173] A. Gabrielli,[20a,20b] A. Gabrielli,[133a,133b] S. Gadatsch,[106] S. Gadomski,[49] G. Gagliardi,[50a,50b] P. Gagnon,[60] C. Galea,[105] B. Galhardo,[125a,125c] E. J. Gallas,[119] V. Gallo,[17] B. J. Gallop,[130] P. Gallus,[127] G. Galster,[36] K. K. Gan,[110] R. P. Gandrajula,[62] J. Gao,[33b,84] Y. S. Gao,[144,f] F. M. Garay Walls,[46] F. Garberson,[177] C. García,[168] J. E. García Navarro,[168] M. Garcia-Sciveres,[15] R. W. Gardner,[31] N. Garelli,[144] V. Garonne,[30] C. Gatti,[47] G. Gaudio,[120a] B. Gaur,[142] L. Gauthier,[94] P. Gauzzi,[133a,133b] I. L. Gavrilenko,[95] C. Gay,[169] G. Gaycken,[21] E. N. Gazis,[10] P. Ge,[33d] Z. Gecse,[169] C. N. P. Gee,[130] D. A. A. Geerts,[106] Ch. Geich-Gimbel,[21] C. Gemme,[50a] A. Gemmell,[53] M. H. Genest,[55] S. Gentile,[133a,133b] M. George,[54] S. George,[76] D. Gerbaudo,[164] A. Gershon,[154] H. Ghazlane,[136b] N. Ghodbane,[34] B. Giacobbe,[20a] S. Giagu,[133a,133b] V. Giangiobbe,[12] P. Giannetti,[123a,123b] F. Gianotti,[30] B. Gibbard,[25] S. M. Gibson,[76] M. Gilchriese,[15] T. P. S. Gillam,[28] D. Gillberg,[30] G. Gilles,[34] D. M. Gingrich,[3,e] N. Giokaris,[9] M. P. Giordani,[165a,165c] R. Giordano,[103a,103b] F. M. Giorgi,[20a] F. M. Giorgi,[16] P. F. Giraud,[137] D. Giugni,[90a] C. Giuliani,[48] M. Giulini,[58b] B. K. Gjelsten,[118] S. Gkaitatzis,[155] I. Gkialas,[155] L. K. Gladilin,[98] C. Glasman,[81] J. Glatzer,[30] P. C. F. Glaysher,[46] A. Glazov,[42] G. L. Glonti,[64] M. Goblirsch-Kolb,[100] J. R. Goddard,[75] J. Godfrey,[143] J. Godlewski,[30] C. Goeringer,[82] S. Goldfarb,[88] T. Golling,[177] D. Golubkov,[129] A. Gomes,[125a,125b,125d] L. S. Gomez Fajardo,[42] R. Gonçalo,[125a] J. Goncalves Pinto Firmino Da Costa,[137] L. Gonella,[21] S. González de la Hoz,[168] G. Gonzalez Parra,[12] S. Gonzalez-Sevilla,[49] L. Goossens,[30] P. A. Gorbounov,[96] H. A. Gordon,[25] I. Gorelov,[104] B. Gorini,[30] E. Gorini,[72a,72b] A. Gorišek,[74] E. Gornicki,[39] A. T. Goshaw,[6] C. Gössling,[43] M. I. Gostkin,[64] M. Gouighri,[136a] D. Goujdami,[136c] M. P. Goulette,[49] A. G. Goussiou,[139] C. Goy,[5] S. Gozpinar,[23] H. M. X. Grabas,[137] L. Graber,[54] I. Grabowska-Bold,[38a] P. Grafström,[20a,20b] K-J. Grahn,[42] J. Gramling,[49] E. Gramstad,[118] S. Grancagnolo,[16] V. Grassi,[149] V. Gratchev,[122] H. M. Gray,[30] E. Graziani,[135a] O. G. Grebenyuk,[122] Z. D. Greenwood,[78,o] K. Gregersen,[77] I. M. Gregor,[42] P. Grenier,[144] J. Griffiths,[8] A. A. Grillo,[138] K. Grimm,[71] S. Grinstein,[12,p] Ph. Gris,[34] Y. V. Grishkevich,[98] J.-F. Grivaz,[116] J. P. Grohs,[44] A. Grohsjean,[42] E. Gross,[173] J. Grosse-Knetter,[54] G. C. Grossi,[134a,134b] J. Groth-Jensen,[173] Z. J. Grout,[150] L. Guan,[33b] J. Guenther,[127] F. Guescini,[49] D. Guest,[177] O. Gueta,[154] C. Guicheney,[34] E. Guido,[50a,50b] T. Guillemin,[116] S. Guindon,[2] U. Gul,[53] C. Gumpert,[44] J. Guo,[35] S. Gupta,[119] P. Gutierrez,[112] N. G. Gutierrez Ortiz,[53] C. Gutschow,[77] N. Guttman,[154] C. Guyot,[137] C. Gwenlan,[119] C. B. Gwilliam,[73] A. Haas,[109] C. Haber,[15] H. K. Hadavand,[8] N. Haddad,[136e] P. Haefner,[21] S. Hageböck,[21] Z. Hajduk,[39] H. Hakobyan,[178] M. Haleem,[42] D. Hall,[119] G. Halladjian,[89] K. Hamacher,[176] P. Hamal,[114] K. Hamano,[170] M. Hamer,[54] A. Hamilton,[146a] S. Hamilton,[162] G. N. Hamity,[146c] P. G. Hamnett,[42] L. Han,[33b] K. Hanagaki,[117] K. Hanawa,[156] M. Hance,[15] P. Hanke,[58a] R. Hanna,[137] J. B. Hansen,[36] J. D. Hansen,[36] P. H. Hansen,[36] K. Hara,[161] A. S. Hard,[174] T. Harenberg,[176] F. Hariri,[116] S. Harkusha,[91] D. Harper,[88] R. D. Harrington,[46] O. M. Harris,[139] P. F. Harrison,[171] F. Hartjes,[106] M. Hasegawa,[66] S. Hasegawa,[102] Y. Hasegawa,[141] A. Hasib,[112] S. Hassani,[137] S. Haug,[17] M. Hauschild,[30] R. Hauser,[89] M. Havranek,[126] C. M. Hawkes,[18] R. J. Hawkings,[30] A. D. Hawkins,[80] T. Hayashi,[161] D. Hayden,[89] C. P. Hays,[119] H. S. Hayward,[73] S. J. Haywood,[130] S. J. Head,[18] T. Heck,[82] V. Hedberg,[80] L. Heelan,[8] S. Heim,[121] T. Heim,[176] B. Heinemann,[15] L. Heinrich,[109] J. Hejbal,[126] L. Helary,[22] C. Heller,[99] M. Heller,[30] S. Hellman,[147a,147b] D. Hellmich,[21] C. Helsens,[30] J. Henderson,[119] R. C. W. Henderson,[71] Y. Heng,[174] C. Hengler,[42] A. Henrichs,[177] A. M. Henriques Correia,[30] S. Henrot-Versille,[116] C. Hensel,[54] G. H. Herbert,[16] Y. Hernández Jiménez,[168] R. Herrberg-Schubert,[16] G. Herten,[48] R. Hertenberger,[99] L. Hervas,[30] G. G. Hesketh,[77] N. P. Hessey,[106] R. Hickling,[75] E. Higón-Rodriguez,[168] E. Hill,[170] J. C. Hill,[28] K. H. Hiller,[42] S. Hillert,[21] S. J. Hillier,[18] I. Hinchliffe,[15] E. Hines,[121] M. Hirose,[158] D. Hirschbuehl,[176] J. Hobbs,[149] N. Hod,[106] M. C. Hodgkinson,[140] P. Hodgson,[140] A. Hoecker,[30] M. R. Hoeferkamp,[104] F. Hoenig,[99] J. Hoffman,[40] D. Hoffmann,[84] M. Hohlfeld,[82] T. R. Holmes,[15] T. M. Hong,[121] L. Hooft van Huysduynen,[109] J-Y. Hostachy,[55] S. Hou,[152] A. Hoummada,[136a] J. Howard,[119] J. Howarth,[42] M. Hrabovsky,[114] I. Hristova,[16] J. Hrivnac,[116] T. Hryn'ova,[5] C. Hsu,[146c] P. J. Hsu,[82] S.-C. Hsu,[139] D. Hu,[35] X. Hu,[88] Y. Huang,[42] Z. Hubacek,[30] F. Hubaut,[84] F. Huegging,[21] T. B. Huffman,[119] E. W. Hughes,[35] G. Hughes,[71] M. Huhtinen,[30] T. A. Hülsing,[82] M. Hurwitz,[15] N. Huseynov,[64,b] J. Huston,[89] J. Huth,[57] G. Iacobucci,[49] G. Iakovidis,[10] I. Ibragimov,[142] L. Iconomidou-Fayard,[116] E. Ideal,[177] P. Iengo,[103a] O. Igonkina,[106] T. Iizawa,[172] Y. Ikegami,[65] K. Ikematsu,[142] M. Ikeno,[65] Y. Ilchenko,[31,q] D. Iliadis,[155] N. Ilic,[159] Y. Inamaru,[66] T. Ince,[100] P. Ioannou,[9] M. Iodice,[135a] K. Iordanidou,[9] V. Ippolito,[57] A. Irles Quiles,[168] C. Isaksson,[167] M. Ishino,[67] M. Ishitsuka,[158] R. Ishmukhametov,[110] C. Issever,[119] S. Istin,[19a] J. M. Iturbe Ponce,[83] R. Iuppa,[134a,134b] J. Ivarsson,[80] W. Iwanski,[39] H. Iwasaki,[65] J. M. Izen,[41] V. Izzo,[103a] B. Jackson,[121] M. Jackson,[73] P. Jackson,[1] M. R. Jaekel,[30] V. Jain,[2] K. Jakobs,[48] S. Jakobsen,[30] T. Jakoubek,[126] J. Jakubek,[127] D. O. Jamin,[152] D. K. Jana,[78] E. Jansen,[77] H. Jansen,[30] J. Janssen,[21] M. Janus,[171] G. Jarlskog,[80] N. Javadov,[64,b] T. Javůrek,[48] L. Jeanty,[15] J. Jejelava,[51a,r] G.-Y. Jeng,[151] D. Jennens,[87] P. Jenni,[48,s] J. Jentzsch,[43] C. Jeske,[171] S. Jézéquel,[5] H. Ji,[174] J. Jia,[149] Y. Jiang,[33b] M. Jimenez Belenguer,[42] S. Jin,[33a] A. Jinaru,[26a] O. Jinnouchi,[158] M. D. Joergensen,[36] K. E. Johansson,[147a,147b] P. Johansson,[140]

K. A. Johns,[7] K. Jon-And,[147a,147b] G. Jones,[171] R. W. L. Jones,[71] T. J. Jones,[73] J. Jongmanns,[58a] P. M. Jorge,[125a,125b] K. D. Joshi,[83] J. Jovicevic,[148] X. Ju,[174] C. A. Jung,[43] R. M. Jungst,[30] P. Jussel,[61] A. Juste Rozas,[12,p] M. Kaci,[168] A. Kaczmarska,[39] M. Kado,[116] H. Kagan,[110] M. Kagan,[144] E. Kajomovitz,[45] C. W. Kalderon,[119] S. Kama,[40] A. Kamenshchikov,[129] N. Kanaya,[156] M. Kaneda,[30] S. Kaneti,[28] V. A. Kantserov,[97] J. Kanzaki,[65] B. Kaplan,[109] A. Kapliy,[31] D. Kar,[53] K. Karakostas,[10] N. Karastathis,[10] M. Karnevskiy,[82] S.N. Karpov,[64] Z.M. Karpova,[64] K. Karthik,[109] V. Kartvelishvili,[71] A. N. Karyukhin,[129] L. Kashif,[174] G. Kasieczka,[58b] R. D. Kass,[110] A. Kastanas,[14] Y. Kataoka,[156] A. Katre,[49] J. Katzy,[42] V. Kaushik,[7] K. Kawagoe,[69] T. Kawamoto,[156] G. Kawamura,[54] S. Kazama,[156] V. F. Kazanin,[108,c] M. Y. Kazarinov,[64] R. Keeler,[170] R. Kehoe,[40] J. S. Keller,[42] J. J. Kempster,[76] H. Keoshkerian,[5] O. Kepka,[126] B. P. Kerševan,[74] S. Kersten,[176] K. Kessoku,[156] J. Keung,[159] F. Khalil-zada,[11] H. Khandanyan,[147a,147b] A. Khanov,[113] A. Khodinov,[97] A. Khomich,[58a] T. J. Khoo,[28] G. Khoriauli,[21] A. Khoroshilov,[176] V. Khovanskiy,[96] E. Khramov,[64] J. Khubua,[51b,t] H. Y. Kim,[8] H. Kim,[147a,147b] S. H. Kim,[161] N. Kimura,[172] O. M. Kind,[16] B. T. King,[73] M. King,[168] R. S. B. King,[119] S. B. King,[169] J. Kirk,[130] A. E. Kiryunin,[100] T. Kishimoto,[66] D. Kisielewska,[38a] F. Kiss,[48] T. Kittelmann,[124] K. Kiuchi,[161] E. Kladiva,[145b] M. Klein,[73] U. Klein,[73] K. Kleinknecht,[82] P. Klimek,[147a,147b] A. Klimentov,[25] R. Klingenberg,[43] J. A. Klinger,[83] T. Klioutchnikova,[30] P. F. Klok,[105] E.-E. Kluge,[58a] P. Kluit,[106] S. Kluth,[100] E. Kneringer,[61] E. B. F. G. Knoops,[84] A. Knue,[53] D. Kobayashi,[158] T. Kobayashi,[156] M. Kobel,[44] M. Kocian,[144] P. Kodys,[128] P. Koevesarki,[21] T. Koffas,[29] E. Koffeman,[106] L. A. Kogan,[119] S. Kohlmann,[176] Z. Kohout,[127] T. Kohriki,[65] T. Koi,[144] H. Kolanoski,[16] I. Koletsou,[5] J. Koll,[89] A. A. Komar,[95,*] Y. Komori,[156] T. Kondo,[65] N. Kondrashova,[42] K. Köneke,[48] A. C. König,[105] S. König,[82] T. Kono,[65,u] R. Konoplich,[109,v] N. Konstantinidis,[77] R. Kopeliansky,[153] S. Koperny,[38a] L. Köpke,[82] A. K. Kopp,[48] K. Korcyl,[39] K. Kordas,[155] A. Korn,[77] A. A. Korol,[108,c] I. Korolkov,[12] E. V. Korolkova,[140] V. A. Korotkov,[129] O. Kortner,[100] S. Kortner,[100] V. V. Kostyukhin,[21] V. M. Kotov,[64] A. Kotwal,[45] C. Kourkoumelis,[9] V. Kouskoura,[155] A. Koutsman,[160a] R. Kowalewski,[170] T. Z. Kowalski,[38a] W. Kozanecki,[137] A. S. Kozhin,[129] V. Kral,[127] V. A. Kramarenko,[98] G. Kramberger,[74] D. Krasnopevtsev,[97] M. W. Krasny,[79] A. Krasznahorkay,[30] J. K. Kraus,[21] A. Kravchenko,[25] S. Kreiss,[109] M. Kretz,[58c] J. Kretzschmar,[73] K. Kreutzfeldt,[52] P. Krieger,[159] K. Kroeninger,[54] H. Kroha,[100] J. Kroll,[121] J. Kroseberg,[21] J. Krstic,[13] U. Kruchonak,[64] H. Krüger,[21] T. Kruker,[17] N. Krumnack,[63] Z. V. Krumshteyn,[64] A. Kruse,[174] M. C. Kruse,[45] M. Kruskal,[22] T. Kubota,[87] S. Kuday,[4a] S. Kuehn,[48] A. Kugel,[58c] A. Kuhl,[138] T. Kuhl,[42] V. Kukhtin,[64] Y. Kulchitsky,[91] S. Kuleshov,[32b] M. Kuna,[133a,133b] J. Kunkle,[121] A. Kupco,[126] H. Kurashige,[66] Y. A. Kurochkin,[91] R. Kurumida,[66] V. Kus,[126] E. S. Kuwertz,[148] M. Kuze,[158] J. Kvita,[114] A. La Rosa,[49] L. La Rotonda,[37a,37b] C. Lacasta,[168] F. Lacava,[133a,133b] J. Lacey,[29] H. Lacker,[16] D. Lacour,[79] V. R. Lacuesta,[168] E. Ladygin,[64] R. Lafaye,[5] B. Laforge,[79] T. Lagouri,[177] S. Lai,[48] H. Laier,[58a] L. Lambourne,[77] S. Lammers,[60] C. L. Lampen,[7] W. Lampl,[7] E. Lançon,[137] U. Landgraf,[48] M. P. J. Landon,[75] V. S. Lang,[58a] A. J. Lankford,[164] F. Lanni,[25] K. Lantzsch,[30] S. Laplace,[79] C. Lapoire,[21] J. F. Laporte,[137] T. Lari,[90a] M. Lassnig,[30] P. Laurelli,[47] W. Lavrijsen,[15] A. T. Law,[138] P. Laycock,[73] O. Le Dortz,[79] E. Le Guirriec,[84] E. Le Menedeu,[12] T. LeCompte,[6] F. Ledroit-Guillon,[55] C. A. Lee,[152] H. Lee,[106] J. S. H. Lee,[117] S. C. Lee,[152] L. Lee,[177] G. Lefebvre,[79] M. Lefebvre,[170] F. Legger,[99] C. Leggett,[15] A. Lehan,[73] M. Lehmacher,[21] G. Lehmann Miotto,[30] X. Lei,[7] W. A. Leight,[29] A. Leisos,[155,w] A. G. Leister,[177] M. A. L. Leite,[24d] R. Leitner,[128] D. Lellouch,[173] B. Lemmer,[54] K. J. C. Leney,[77] T. Lenz,[21] B. Lenzi,[30] R. Leone,[7] S. Leone,[123a,123b] K. Leonhardt,[44] C. Leonidopoulos,[46] S. Leontsinis,[10] C. Leroy,[94] C. G. Lester,[28] C. M. Lester,[121] M. Levchenko,[122] J. Levêque,[5] D. Levin,[88] L. J. Levinson,[173] M. Levy,[18] A. Lewis,[119] G. H. Lewis,[109] A. M. Leyko,[21] M. Leyton,[41] B. Li,[33b,x] B. Li,[84] H. Li,[149] H. L. Li,[31] L. Li,[45] L. Li,[33e] S. Li,[45] Y. Li,[33c,y] Z. Liang,[138] H. Liao,[34] B. Liberti,[134a] P. Lichard,[30] K. Lie,[166] J. Liebal,[21] W. Liebig,[14] C. Limbach,[21] A. Limosani,[87] S. C. Lin,[152,z] T. H. Lin,[82] F. Linde,[106] B. E. Lindquist,[149] J. T. Linnemann,[89] E. Lipeles,[121] A. Lipniacka,[14] M. Lisovyi,[42] T. M. Liss,[166] D. Lissauer,[25] A. Lister,[169] A. M. Litke,[138] B. Liu,[152,aa] D. Liu,[152] J. B. Liu,[33b] K. Liu,[33b,ab] L. Liu,[88] M. Liu,[45] M. Liu,[33b] Y. Liu,[33b] M. Livan,[120a,120b] S. S. A. Livermore,[119] A. Lleres,[55] J. Llorente Merino,[81] S. L. Lloyd,[75] F. Lo Sterzo,[152] E. Lobodzinska,[42] P. Loch,[7] W. S. Lockman,[138] F. K. Loebinger,[83] A. E. Loevschall-Jensen,[36] A. Loginov,[177] T. Lohse,[16] K. Lohwasser,[42] M. Lokajicek,[126] V. P. Lombardo,[5] B. A. Long,[22] J. D. Long,[88] R. E. Long,[71] L. Lopes,[125a] D. Lopez Mateos,[57] B. Lopez Paredes,[140] I. Lopez Paz,[12] J. Lorenz,[99] N. Lorenzo Martinez,[60] M. Losada,[163] P. Loscutoff,[15] X. Lou,[41] A. Lounis,[116] J. Love,[6] P. A. Love,[71] A. J. Lowe,[144,f] N. Lu,[88] H. J. Lubatti,[139] C. Luci,[133a,133b] A. Lucotte,[55] F. Luehring,[60] W. Lukas,[61] L. Luminari,[133a] O. Lundberg,[147a,147b] B. Lund-Jensen,[148] M. Lungwitz,[82] D. Lynn,[25] R. Lysak,[126] E. Lytken,[80] H. Ma,[25] L. L. Ma,[33d] G. Maccarrone,[47] A. Macchiolo,[100] J. Machado Miguens,[125a,125b] D. Macina,[30] D. Madaffari,[84] R. Madar,[48] H. J. Maddocks,[71] W. F. Mader,[44] A. Madsen,[167] T. Maeno,[25] M. Maeno Kataoka,[8] E. Magradze,[54] K. Mahboubi,[48] J. Mahlstedt,[106] S. Mahmoud,[73] C. Maiani,[137] C. Maidantchik,[24a] A. A. Maier,[100] A. Maio,[125a,125b,125d] S. Majewski,[115] Y. Makida,[65] N. Makovec,[116] P. Mal,[137,ac] B. Malaescu,[79] Pa. Malecki,[39] V. P. Maleev,[122] F. Malek,[55] U. Mallik,[62] D. Malon,[6] C. Malone,[144] S. Maltezos,[10] V. M. Malyshev,[108] S. Malyukov,[30] J. Mamuzic,[13] B. Mandelli,[30] L. Mandelli,[90a] I. Mandić,[74] R. Mandrysch,[62] J. Maneira,[125a,125b] A. Manfredini,[100] L. Manhaes de Andrade Filho,[24b] J. Manjarres Ramos,[160b] A. Mann,[99] P. M. Manning,[138] A. Manousakis-Katsikakis,[9] B. Mansoulie,[137] R. Mantifel,[86] L. Mapelli,[30] L. March,[146c] J. F. Marchand,[29] G. Marchiori,[79] M. Marcisovsky,[126] C. P. Marino,[170] M. Marjanovic,[13] C. N. Marques,[125a] F. Marroquim,[24a] S. P. Marsden,[83] Z. Marshall,[15] L. F. Marti,[17] S. Marti-Garcia,[168] B. Martin,[30] B. Martin,[89] T. A. Martin,[171] V. J. Martin,[46] B. Martin dit Latour,[14] H. Martinez,[137] M. Martinez,[12,p] S. Martin-Haugh,[130] A. C. Martyniuk,[77] M. Marx,[139] F. Marzano,[133a] A. Marzin,[30] L. Masetti,[82] T. Mashimo,[156] R. Mashinistov,[95] J. Masik,[83] A. L. Maslennikov,[108,c] I. Massa,[20a,20b] L. Massa,[20a,20b] N. Massol,[5] P. Mastrandrea,[149] A. Mastroberardino,[37a,37b] T. Masubuchi,[156] P. Mättig,[176] J. Mattmann,[82] J. Maurer,[26a] S. J. Maxfield,[73] D. A. Maximov,[108,c] R. Mazini,[152] L. Mazzaferro,[134a,134b] G. Mc Goldrick,[159] S. P. Mc Kee,[88]

A. McCarn,[88] R. L. McCarthy,[149] T. G. McCarthy,[29] N. A. McCubbin,[130] K. W. McFarlane,[56,*] J. A. Mcfayden,[77] G. Mchedlidze,[54] S. J. McMahon,[130] R. A. McPherson,[170,1] A. Meade,[85] J. Mechnich,[106] M. Medinnis,[42] S. Meehan,[31] S. Mehlhase,[99] A. Mehta,[73] K. Meier,[58a] C. Meineck,[99] B. Meirose,[80] C. Melachrinos,[31] B. R. Mellado Garcia,[146c] F. Meloni,[17] A. Mengarelli,[20a,20b] S. Menke,[100] E. Meoni,[162] K. M. Mercurio,[57] S. Mergelmeyer,[21] N. Meric,[137] P. Mermod,[49] L. Merola,[103a,103b] C. Meroni,[90a] F. S. Merritt,[31] H. Merritt,[110] A. Messina,[30,ad] J. Metcalfe,[25] A. S. Mete,[164] C. Meyer,[82] C. Meyer,[121] J-P. Meyer,[137] J. Meyer,[30] R. P. Middleton,[130] S. Migas,[73] L. Mijović,[21] G. Mikenberg,[173] M. Mikestikova,[126] M. Mikuž,[74] A. Milic,[30] D. W. Miller,[31] C. Mills,[46] A. Milov,[173] D. A. Milstead,[147a,147b] D. Milstein,[173] A. A. Minaenko,[129] I. A. Minashvili,[64] A. I. Mincer,[109] B. Mindur,[38a] M. Mineev,[64] Y. Ming,[174] L. M. Mir,[12] G. Mirabelli,[133a] T. Mitani,[172] J. Mitrevski,[99] V. A. Mitsou,[168] S. Mitsui,[65] A. Miucci,[49] P. S. Miyagawa,[140] J. U. Mjörnmark,[80] T. Moa,[147a,147b] K. Mochizuki,[84] S. Mohapatra,[35] W. Mohr,[48] S. Molander,[147a,147b] R. Moles-Valls,[168] K. Mönig,[42] C. Monini,[55] J. Monk,[36] E. Monnier,[84] J. Montejo Berlingen,[12] F. Monticelli,[70] S. Monzani,[133a,133b] R. W. Moore,[3] A. Moraes,[53] N. Morange,[62] D. Moreno,[82] M. Moreno Llácer,[54] P. Morettini,[50a] M. Morgenstern,[44] M. Morii,[57] S. Moritz,[82] A. K. Morley,[148] G. Mornacchi,[30] J. D. Morris,[75] L. Morvaj,[102] H. G. Moser,[100] M. Mosidze,[51b] J. Moss,[110] K. Motohashi,[158] R. Mount,[144] E. Mountricha,[25] S. V. Mouraviev,[95,*] E. J. W. Moyse,[85] S. Muanza,[84] R. D. Mudd,[18] F. Mueller,[58a] J. Mueller,[124] K. Mueller,[21] T. Mueller,[28] T. Mueller,[82] D. Muenstermann,[49] Y. Munwes,[154] J. A. Murillo Quijada,[18] W. J. Murray,[171,130] H. Musheghyan,[54] E. Musto,[153] A. G. Myagkov,[129,ae] M. Myska,[127] O. Nackenhorst,[54] J. Nadal,[54] K. Nagai,[61] R. Nagai,[158] Y. Nagai,[84] K. Nagano,[65] A. Nagarkar,[110] Y. Nagasaka,[59] M. Nagel,[100] A. M. Nairz,[30] Y. Nakahama,[30] K. Nakamura,[65] T. Nakamura,[156] I. Nakano,[111] H. Namasivayam,[41] G. Nanava,[21] R. Narayan,[58b] T. Nattermann,[21] T. Naumann,[42] G. Navarro,[163] R. Nayyar,[7] H. A. Neal,[88] P. Yu. Nechaeva,[95] T. J. Neep,[83] P. D. Nef,[144] A. Negri,[120a,120b] G. Negri,[30] M. Negrini,[20a] S. Nektarijevic,[49] A. Nelson,[164] T. K. Nelson,[144] S. Nemecek,[126] P. Nemethy,[109] A. A. Nepomuceno,[24a] M. Nessi,[30,af] M. S. Neubauer,[166] M. Neumann,[176] R. M. Neves,[109] P. Nevski,[25] P. R. Newman,[18] D. H. Nguyen,[6] R. B. Nickerson,[119] R. Nicolaidou,[137] B. Nicquevert,[30] J. Nielsen,[138] N. Nikiforou,[35] A. Nikiforov,[16] V. Nikolaenko,[129,ae] I. Nikolic-Audit,[79] K. Nikolics,[49] K. Nikolopoulos,[18] P. Nilsson,[8] Y. Ninomiya,[156] A. Nisati,[133a] R. Nisius,[100] T. Nobe,[158] L. Nodulman,[6] M. Nomachi,[117] I. Nomidis,[29] S. Norberg,[112] M. Nordberg,[30] O. Novgorodova,[44] S. Nowak,[100] M. Nozaki,[65] L. Nozka,[114] K. Ntekas,[10] G. Nunes Hanninger,[87] T. Nunnemann,[99] E. Nurse,[77] F. Nuti,[87] B. J. O'Brien,[46] F. O'grady,[7] D. C. O'Neil,[143] V. O'Shea,[53] F. G. Oakham,[29,e] H. Oberlack,[100] T. Obermann,[21] J. Ocariz,[79] A. Ochi,[66] I. Ochoa,[77] S. Oda,[69] S. Odaka,[65] H. Ogren,[60] A. Oh,[83] S. H. Oh,[45] C. C. Ohm,[15] H. Ohman,[167] W. Okamura,[117] H. Okawa,[25] Y. Okumura,[31] T. Okuyama,[156] A. Olariu,[26a] A. G. Olchevski,[64] S. A. Olivares Pino,[46] D. Oliveira Damazio,[25] E. Oliver Garcia,[168] A. Olszewski,[39] J. Olszowska,[39] A. Onofre,[125a,125e] P. U. E. Onyisi,[31,q] C. J. Oram,[160a] M. J. Oreglia,[31] Y. Oren,[154] D. Orestano,[135a,135b] N. Orlando,[72a,72b] C. Oropeza Barrera,[53] R. S. Orr,[159] B. Osculati,[50a,50b] R. Ospanov,[121] G. Otero y Garzon,[27] H. Otono,[69] M. Ouchrif,[136d] E. A. Ouellette,[170] F. Ould-Saada,[118] A. Ouraou,[137] K. P. Oussoren,[106] Q. Ouyang,[33a] A. Ovcharova,[15] M. Owen,[83] V. E. Ozcan,[19a] N. Ozturk,[8] K. Pachal,[119] A. Pacheco Pages,[12] C. Padilla Aranda,[12] M. Pagáčová,[48] S. Pagan Griso,[15] E. Paganis,[140] C. Pahl,[100] F. Paige,[25] P. Pais,[85] K. Pajchel,[118] G. Palacino,[160b] S. Palestini,[30] M. Palka,[38b] D. Pallin,[34] A. Palma,[125a,125b] J. D. Palmer,[18] Y. B. Pan,[174] E. Panagiotopoulou,[10] J. G. Panduro Vazquez,[76] P. Pani,[106] N. Panikashvili,[88] S. Panitkin,[25] D. Pantea,[26a] L. Paolozzi,[134a,134b] Th. D. Papadopoulou,[10] K. Papageorgiou,[155] A. Paramonov,[6] D. Paredes Hernandez,[34] M. A. Parker,[28] F. Parodi,[50a,50b] J. A. Parsons,[35] U. Parzefall,[48] E. Pasqualucci,[133a] S. Passaggio,[50a] A. Passeri,[135a] F. Pastore,[135a,135b,*] Fr. Pastore,[76] G. Pásztor,[29] S. Pataraia,[176] N. D. Patel,[151] J. R. Pater,[83] S. Patricelli,[103a,103b] T. Pauly,[30] J. Pearce,[170] M. Pedersen,[118] S. Pedraza Lopez,[168] R. Pedro,[125a,125b] S. V. Peleganchuk,[108,c] D. Pelikan,[167] H. Peng,[33b] B. Penning,[31] J. Penwell,[60] D. V. Perepelitsa,[25] E. Perez Codina,[160a] M. T. Pérez García-Estañ,[168] V. Perez Reale,[35] L. Perini,[90a,90b] H. Pernegger,[30] R. Perrino,[72a] R. Peschke,[42] V. D. Peshekhonov,[64] K. Peters,[30] R. F. Y. Peters,[83] B. A. Petersen,[30] T. C. Petersen,[36] E. Petit,[42] A. Petridis,[147a,147b] C. Petridou,[155] E. Petrolo,[133a] F. Petrucci,[135a,135b] N. E. Pettersson,[158] R. Pezoa,[32b] P. W. Phillips,[130] G. Piacquadio,[144] E. Pianori,[171] A. Picazio,[49] E. Piccaro,[75] M. Piccinini,[20a,20b] R. Piegaia,[27] D. T. Pignotti,[110] J. E. Pilcher,[31] A. D. Pilkington,[77] J. Pina,[125a,125b,125d] M. Pinamonti,[165a,165c,ag] A. Pinder,[119] J. L. Pinfold,[3] A. Pingel,[36] B. Pinto,[125a] S. Pires,[79] M. Pitt,[173] C. Pizio,[90a,90b] L. Plazak,[145a] M.-A. Pleier,[25] V. Pleskot,[128] E. Plotnikova,[64] P. Plucinski,[147a,147b] S. Poddar,[58a] F. Podlyski,[34] R. Poettgen,[82] L. Poggioli,[116] D. Pohl,[21] M. Pohl,[49] G. Polesello,[120a] A. Policicchio,[37a,37b] R. Polifka,[159] A. Polini,[20a] C. S. Pollard,[45] V. Polychronakos,[25] K. Pommès,[30] L. Pontecorvo,[133a] B. G. Pope,[89] G. A. Popeneciu,[26b] D. S. Popovic,[13] A. Poppleton,[30] X. Portell Bueso,[12] S. Pospisil,[127] K. Potamianos,[15] I. N. Potrap,[64] C. J. Potter,[150] C. T. Potter,[115] G. Poulard,[30] J. Poveda,[60] V. Pozdnyakov,[64] P. Pralavorio,[84] A. Pranko,[15] S. Prasad,[30] R. Pravahan,[8] S. Prell,[63] D. Price,[83] J. Price,[73] L. E. Price,[6] D. Prieur,[124] M. Primavera,[72a] M. Proissl,[46] K. Prokofiev,[47] F. Prokoshin,[32b] E. Protopapadaki,[137] S. Protopopescu,[25] J. Proudfoot,[6] M. Przybycien,[38a] H. Przysiezniak,[5] E. Ptacek,[115] D. Puddu,[135a,135b] E. Pueschel,[85] D. Puldon,[149] M. Purohit,[25,ah] P. Puzo,[116] J. Qian,[88] G. Qin,[53] Y. Qin,[83] A. Quadt,[54] D. R. Quarrie,[15] W. B. Quayle,[165a,165b] M. Queitsch-Maitland,[83] D. Quilty,[53] A. Qureshi,[160b] V. Radeka,[25] V. Radescu,[42] S. K. Radhakrishnan,[149] P. Radloff,[115] P. Rados,[87] F. Ragusa,[90a,90b] G. Rahal,[179] S. Rajagopalan,[25] M. Rammensee,[30] A. S. Randle-Conde,[40] C. Rangel-Smith,[167] K. Rao,[164] F. Rauscher,[99] T. C. Rave,[48] T. Ravenscroft,[53] M. Raymond,[30] A. L. Read,[118] N. P. Readioff,[73] D. M. Rebuzzi,[120a,120b] A. Redelbach,[175] G. Redlinger,[25] R. Reece,[138] K. Reeves,[41] L. Rehnisch,[16] H. Reisin,[27] M. Relich,[164] C. Rembser,[30] H. Ren,[33a] Z. L. Ren,[152] A. Renaud,[116] M. Rescigno,[133a] S. Resconi,[90a] O. L. Rezanova,[108,c] P. Reznicek,[128] R. Rezvani,[94] R. Richter,[100] M. Ridel,[79] P. Rieck,[16] J. Rieger,[54] M. Rijssenbeek,[149] A. Rimoldi,[120a,120b] L. Rinaldi,[20a] E. Ritsch,[61] I. Riu,[12] F. Rizatdinova,[113] E. Rizvi,[75]

S. H. Robertson,[86,1] A. Robichaud-Veronneau,[86] D. Robinson,[28] J. E. M. Robinson,[83] A. Robson,[53] C. Roda,[123a,123b] L. Rodrigues,[30] S. Roe,[30] O. Røhne,[118] S. Rolli,[162] A. Romaniouk,[97] M. Romano,[20a,20b] E. Romero Adam,[168] N. Rompotis,[139] M. Ronzani,[48] L. Roos,[79] E. Ros,[168] S. Rosati,[133a] K. Rosbach,[49] M. Rose,[76] P. Rose,[138] P. L. Rosendahl,[14] O. Rosenthal,[142] V. Rossetti,[147a,147b] E. Rossi,[103a,103b] L. P. Rossi,[50a] R. Rosten,[139] M. Rotaru,[26a] I. Roth,[173] J. Rothberg,[139] D. Rousseau,[116] C. R. Royon,[137] A. Rozanov,[84] Y. Rozen,[153] X. Ruan,[146c] F. Rubbo,[12] I. Rubinskiy,[42] V. I. Rud,[98] C. Rudolph,[44] M. S. Rudolph,[159] F. Rühr,[48] A. Ruiz-Martinez,[30] Z. Rurikova,[48] N. A. Rusakovich,[64] A. Ruschke,[99] J. P. Rutherfoord,[7] N. Ruthmann,[48] Y. F. Ryabov,[122] M. Rybar,[128] G. Rybkin,[116] N. C. Ryder,[119] A. F. Saavedra,[151] S. Sacerdoti,[27] A. Saddique,[3] I. Sadeh,[154] H. F-W. Sadrozinski,[138] R. Sadykov,[64] F. Safai Tehrani,[133a] H. Sakamoto,[156] Y. Sakurai,[172] G. Salamanna,[135a,135b] A. Salamon,[134a] M. Saleem,[112] D. Salek,[106] P. H. Sales De Bruin,[139] D. Salihagic,[100] A. Salnikov,[144] J. Salt,[168] D. Salvatore,[37a,37b] F. Salvatore,[150] A. Salvucci,[105] A. Salzburger,[30] D. Sampsonidis,[155] A. Sanchez,[103a,103b] J. Sánchez,[168] V. Sanchez Martinez,[168] H. Sandaker,[14] R. L. Sandbach,[75] H. G. Sander,[82] M. P. Sanders,[99] M. Sandhoff,[176] T. Sandoval,[28] C. Sandoval,[163] R. Sandstroem,[100] D. P. C. Sankey,[130] A. Sansoni,[47] C. Santoni,[34] R. Santonico,[134a,134b] H. Santos,[125a] I. Santoyo Castillo,[150] K. Sapp,[124] A. Sapronov,[64] J. G. Saraiva,[125a,125d] B. Sarrazin,[21] G. Sartisohn,[176] O. Sasaki,[65] Y. Sasaki,[156] G. Sauvage,[5,*] E. Sauvan,[5] P. Savard,[159,e] D. O. Savu,[30] C. Sawyer,[119] L. Sawyer,[78,o] D. H. Saxon,[53] J. Saxon,[121] C. Sbarra,[20a] A. Sbrizzi,[3] T. Scanlon,[77] D. A. Scannicchio,[164] M. Scarcella,[151] V. Scarfone,[37a,37b] J. Schaarschmidt,[173] P. Schacht,[100] D. Schaefer,[30] R. Schaefer,[42] S. Schaepe,[21] S. Schaetzel,[58b] U. Schäfer,[82] A. C. Schaffer,[116] D. Schaile,[99] R. D. Schamberger,[149] V. Scharf,[58a] V. A. Schegelsky,[122] D. Scheirich,[128] M. Schernau,[164] M. I. Scherzer,[35] C. Schiavi,[50a,50b] J. Schieck,[99] C. Schillo,[48] M. Schioppa,[37a,37b] S. Schlenker,[30] E. Schmidt,[48] K. Schmieden,[30] C. Schmitt,[82] S. Schmitt,[58b] B. Schneider,[17] Y. J. Schnellbach,[73] U. Schnoor,[44] L. Schoeffel,[137] A. Schoening,[58b] B. D. Schoenrock,[89] A. L. S. Schorlemmer,[54] M. Schott,[82] D. Schouten,[160a] J. Schovancova,[25] S. Schramm,[159] M. Schreyer,[175] C. Schroeder,[82] N. Schuh,[82] M. J. Schultens,[21] H.-C. Schultz-Coulon,[58a] H. Schulz,[16] M. Schumacher,[48] B. A. Schumm,[138] Ph. Schune,[137] C. Schwanenberger,[83] A. Schwartzman,[144] Ph. Schwegler,[100] Ph. Schwemling,[137] R. Schwienhorst,[89] J. Schwindling,[137] T. Schwindt,[21] M. Schwoerer,[5] F. G. Sciacca,[17] E. Scifo,[116] G. Sciolla,[23] W. G. Scott,[130] F. Scuri,[123a,123b] F. Scutti,[21] J. Searcy,[88] G. Sedov,[42] E. Sedykh,[122] S. C. Seidel,[104] A. Seiden,[138] F. Seifert,[127] J. M. Seixas,[24a] G. Sekhniaidze,[103a] S. J. Sekula,[40] K. E. Selbach,[46] D. M. Seliverstov,[122,*] G. Sellers,[73] N. Semprini-Cesari,[20a,20b] C. Serfon,[30] L. Serin,[116] L. Serkin,[54] T. Serre,[84] R. Seuster,[160a] H. Severini,[112] T. Sfiligoj,[74] F. Sforza,[100] A. Sfyrla,[30] E. Shabalina,[54] M. Shamim,[115] L. Y. Shan,[33a] R. Shang,[166] J. T. Shank,[22] M. Shapiro,[15] P. B. Shatalov,[96] K. Shaw,[165a,165b] C. Y. Shehu,[150] P. Sherwood,[77] L. Shi,[152,ai] S. Shimizu,[66] C. O. Shimmin,[164] M. Shimojima,[101] M. Shiyakova,[64] A. Shmeleva,[95] M. J. Shochet,[31] D. Short,[119] S. Shrestha,[63] E. Shulga,[97] M. A. Shupe,[7] S. Shushkevich,[42] P. Sicho,[126] O. Sidiropoulou,[155] D. Sidorov,[113] A. Sidoti,[133a] F. Siegert,[44] Dj. Sijacki,[13] J. Silva,[125a,125d] Y. Silver,[154] D. Silverstein,[144] S. B. Silverstein,[147a] V. Simak,[127] O. Simard,[5] Lj. Simic,[13] S. Simion,[116] E. Simioni,[82] B. Simmons,[77] R. Simoniello,[90a,90b] M. Simonyan,[36] P. Sinervo,[159] N. B. Sinev,[115] V. Sipica,[142] G. Siragusa,[175] A. Sircar,[78] A. N. Sisakyan,[64,*] S. Yu. Sivoklokov,[98] J. Sjölin,[147a,147b] T. B. Sjursen,[14] H. P. Skottowe,[57] K. Yu. Skovpen,[108] P. Skubic,[112] M. Slater,[18] T. Slavicek,[127] K. Sliwa,[162] V. Smakhtin,[173] B. H. Smart,[46] L. Smestad,[14] S. Yu. Smirnov,[97] Y. Smirnov,[97] L. N. Smirnova,[98,aj] O. Smirnova,[80] K. M. Smith,[53] M. Smizanska,[71] K. Smolek,[127] A. A. Snesarev,[95] G. Snidero,[75] S. Snyder,[25] R. Sobie,[170,1] F. Socher,[44] A. Soffer,[154] D. A. Soh,[152,ai] C. A. Solans,[30] M. Solar,[127] J. Solc,[127] E. Yu. Soldatov,[97] U. Soldevila,[168] A. A. Solodkov,[129] A. Soloshenko,[64] O. V. Solovyanov,[129] V. Solovyev,[122] P. Sommer,[48] H. Y. Song,[33b] N. Soni,[1] A. Sood,[15] A. Sopczak,[127] B. Sopko,[127] V. Sopko,[127] V. Sorin,[12] M. Sosebee,[8] R. Soualah,[165a,165c] P. Soueid,[94] A. M. Soukharev,[108,c] D. South,[42] S. Spagnolo,[72a,72b] F. Spanò,[76] W. R. Spearman,[57] F. Spettel,[100] R. Spighi,[20a] G. Spigo,[30] L. A. Spiller,[87] M. Spousta,[128] T. Spreitzer,[159] B. Spurlock,[8] R. D. St. Denis,[53,*] S. Staerz,[44] J. Stahlman,[121] R. Stamen,[58a] S. Stamm,[16] E. Stanecka,[39] R. W. Stanek,[6] C. Stanescu,[135a] M. Stanescu-Bellu,[42] M. M. Stanitzki,[42] S. Stapnes,[118] E. A. Starchenko,[129] J. Stark,[55] P. Staroba,[126] P. Starovoitov,[42] R. Staszewski,[39] P. Stavina,[145a,*] P. Steinberg,[25] B. Stelzer,[143] H. J. Stelzer,[30] O. Stelzer-Chilton,[160a] H. Stenzel,[52] S. Stern,[100] G. A. Stewart,[53] J. A. Stillings,[21] M. C. Stockton,[86] M. Stoebe,[86] G. Stoicea,[26a] P. Stolte,[54] S. Stonjek,[100] A. R. Stradling,[8] A. Straessner,[44] M. E. Stramaglia,[17] J. Strandberg,[148] S. Strandberg,[147a,147b] A. Strandlie,[118] E. Strauss,[144] M. Strauss,[112] P. Strizenec,[145b] R. Ströhmer,[175] D. M. Strom,[115] R. Stroynowski,[40] S. A. Stucci,[17] B. Stugu,[14] N. A. Styles,[42] D. Su,[144] J. Su,[124] R. Subramaniam,[78] A. Succurro,[12] Y. Sugaya,[117] C. Suhr,[107] M. Suk,[127] V. V. Sulin,[95] S. Sultansoy,[4c] T. Sumida,[67] S. Sun,[57] X. Sun,[33a] J. E. Sundermann,[48] K. Suruliz,[140] G. Susinno,[37a,37b] M. R. Sutton,[150] Y. Suzuki,[65] M. Svatos,[126] S. Swedish,[169] M. Swiatlowski,[144] I. Sykora,[145a] T. Sykora,[128] D. Ta,[89] C. Taccini,[135a,135b] K. Tackmann,[42] J. Taenzer,[159] A. Taffard,[164] R. Tafirout,[160a] N. Taiblum,[154] H. Takai,[25] R. Takashima,[68] H. Takeda,[66] T. Takeshita,[141] Y. Takubo,[65] M. Talby,[84] A. A. Talyshev,[108,c] J. Y. C. Tam,[175] K. G. Tan,[87] J. Tanaka,[156] R. Tanaka,[116] S. Tanaka,[132] S. Tanaka,[65] A.J. Tanasijczuk,[143] B. B. Tannenwald,[110] N. Tannoury,[21] S. Tapprogge,[82] S. Tarem,[153] F. Tarrade,[29] G. F. Tartarelli,[90a] P. Tas,[128] M. Tasevsky,[126] T. Tashiro,[67] E. Tassi,[37a,37b] A. Tavares Delgado,[125a,125b] Y. Tayalati,[136d] F. E. Taylor,[93] G. N. Taylor,[87] W. Taylor,[160b] F. A. Teischinger,[30] M. Teixeira Dias Castanheira,[75] P. Teixeira-Dias,[76] K. K. Temming,[48] H. Ten Kate,[30] P. K. Teng,[152] J. J. Teoh,[117] S. Terada,[65] K. Terashi,[156] J. Terron,[81] S. Terzo,[100] M. Testa,[47] R. J. Teuscher,[159,1] J. Therhaag,[21] T. Theveneaux-Pelzer,[34] J. P. Thomas,[18] J. Thomas-Wilsker,[76] E. N. Thompson,[35] P. D. Thompson,[18] P. D. Thompson,[159] R. J. Thompson,[83] A. S. Thompson,[53] L. A. Thomsen,[36] E. Thomson,[121] M. Thomson,[28] W. M. Thong,[87] R. P. Thun,[88,*] F. Tian,[35] M. J. Tibbetts,[15] V. O. Tikhomirov,[95,ak] Yu. A. Tikhonov,[108,c] S. Timoshenko,[97] E. Tiouchichine,[84] P. Tipton,[177] S. Tisserant,[84] T. Todorov,[5,*] S. Todorova-Nova,[128] B. Toggerson,[7] J. Tojo,[69] S. Tokár,[145a] K. Tokushuku,[65] K. Tollefson,[89]

L. Tomlinson,[83] M. Tomoto,[102] L. Tompkins,[31] K. Toms,[104] N. D. Topilin,[64] E. Torrence,[115] H. Torres,[143] E. Torró Pastor,[168] J. Toth,[84,al] F. Touchard,[84] D. R. Tovey,[140] H. L. Tran,[116] T. Trefzger,[175] L. Tremblet,[30] A. Tricoli,[30] I. M. Trigger,[160a] S. Trincaz-Duvoid,[79] M. F. Tripiana,[12] W. Trischuk,[159] B. Trocmé,[55] C. Troncon,[90a] M. Trottier-McDonald,[143] M. Trovatelli,[135a,135b] P. True,[89] M. Trzebinski,[39] A. Trzupek,[39] C. Tsarouchas,[30] J. C-L. Tseng,[119] P. V. Tsiareshka,[91] D. Tsionou,[137] G. Tsipolitis,[10] N. Tsirintanis,[9] S. Tsiskaridze,[12] V. Tsiskaridze,[48] E. G. Tskhadadze,[51a] I. I. Tsukerman,[96] V. Tsulaia,[15] S. Tsuno,[65] D. Tsybychev,[149] A. Tudorache,[26a] V. Tudorache,[26a] A. N. Tuna,[121] S. A. Tupputi,[20a,20b] S. Turchikhin,[98,aj] D. Turecek,[127] R. Turra,[90a,90b] P. M. Tuts,[35] A. Tykhonov,[49] M. Tylmad,[147a,147b] M. Tyndel,[130] K. Uchida,[21] I. Ueda,[156] R. Ueno,[29] M. Ughetto,[84] M. Ugland,[14] M. Uhlenbrock,[21] F. Ukegawa,[161] G. Unal,[30] A. Undrus,[25] G. Unel,[164] F. C. Ungaro,[48] Y. Unno,[65] C. Unverdorben,[99] D. Urbaniec,[35] P. Urquijo,[87] G. Usai,[8] A. Usanova,[61] L. Vacavant,[84] V. Vacek,[127] B. Vachon,[86] N. Valencic,[106] S. Valentinetti,[20a,20b] A. Valero,[168] L. Valery,[34] S. Valkar,[128] E. Valladolid Gallego,[168] S. Vallecorsa,[49] J. A. Valls Ferrer,[168] W. Van Den Wollenberg,[106] P. C. Van Der Deijl,[106] R. van der Geer,[106] H. van der Graaf,[106] R. Van Der Leeuw,[106] D. van der Ster,[30] N. van Eldik,[30] P. van Gemmeren,[6] J. Van Nieuwkoop,[143] I. van Vulpen,[106] M. C. van Woerden,[30] M. Vanadia,[133a,133b] W. Vandelli,[30] R. Vanguri,[121] A. Vaniachine,[6] F. Vannucci,[79] G. Vardanyan,[178] R. Vari,[133a] E. W. Varnes,[7] T. Varol,[85] D. Varouchas,[79] A. Vartapetian,[8] K. E. Varvell,[151] F. Vazeille,[34] T. Vazquez Schroeder,[54] J. Veatch,[7] F. Veloso,[125a,125c] T. Velz,[21] S. Veneziano,[133a] A. Ventura,[72a,72b] D. Ventura,[85] M. Venturi,[170] N. Venturi,[159] A. Venturini,[23] V. Vercesi,[120a] M. Verducci,[133a,133b] W. Verkerke,[106] J. C. Vermeulen,[106] A. Vest,[44] M. C. Vetterli,[143,e] O. Viazlo,[80] I. Vichou,[166] T. Vickey,[146c,am] O. E. Vickey Boeriu,[146c] G. H. A. Viehhauser,[119] S. Viel,[169] R. Vigne,[30] M. Villa,[20a,20b] M. Villaplana Perez,[90a,90b] E. Vilucchi,[47] M. G. Vincter,[29] V. B. Vinogradov,[64] J. Virzi,[15] I. Vivarelli,[150] F. Vives Vaque,[3] S. Vlachos,[10] D. Vladoiu,[99] M. Vlasak,[127] A. Vogel,[21] M. Vogel,[32a] P. Vokac,[127] G. Volpi,[123a,123b] M. Volpi,[87] H. von der Schmitt,[100] H. von Radziewski,[48] E. von Toerne,[21] V. Vorobel,[128] K. Vorobev,[97] M. Vos,[168] R. Voss,[30] J. H. Vossebeld,[73] N. Vranjes,[137] M. Vranjes Milosavljevic,[106] V. Vrba,[126] M. Vreeswijk,[106] T. Vu Anh,[48] R. Vuillermet,[30] I. Vukotic,[31] Z. Vykydal,[127] P. Wagner,[21] W. Wagner,[176] H. Wahlberg,[70] S. Wahrmund,[44] J. Wakabayashi,[102] J. Walder,[71] R. Walker,[99] W. Walkowiak,[142] R. Wall,[177] P. Waller,[73] B. Walsh,[177] C. Wang,[152,an] C. Wang,[45] F. Wang,[174] H. Wang,[15] H. Wang,[40] J. Wang,[42] J. Wang,[33a] K. Wang,[86] R. Wang,[104] S. M. Wang,[152] T. Wang,[21] X. Wang,[177] C. Wanotayaroj,[115] A. Warburton,[86] C. P. Ward,[28] D. R. Wardrope,[77] M. Warsinsky,[48] A. Washbrook,[46] C. Wasicki,[42] P. M. Watkins,[18] A. T. Watson,[18] I. J. Watson,[151] M. F. Watson,[18] G. Watts,[139] S. Watts,[83] B. M. Waugh,[77] S. Webb,[83] M. S. Weber,[17] S. W. Weber,[175] J. S. Webster,[31] A. R. Weidberg,[119] P. Weigell,[100] B. Weinert,[60] J. Weingarten,[54] C. Weiser,[48] H. Weits,[106] P. S. Wells,[30] T. Wenaus,[25] D. Wendland,[16] Z. Weng,[152,ai] T. Wengler,[30] S. Wenig,[30] N. Wermes,[21] M. Werner,[48] P. Werner,[30] M. Wessels,[58a] J. Wetter,[162] K. Whalen,[29] A. White,[8] M. J. White,[1] R. White,[32b] S. White,[123a,123b] D. Whiteson,[164] D. Wicke,[176] F. J. Wickens,[130] W. Wiedenmann,[174] M. Wielers,[130] P. Wienemann,[21] C. Wiglesworth,[36] L. A. M. Wiik-Fuchs,[21] P. A. Wijeratne,[77] A. Wildauer,[100] M. A. Wildt,[42,ao] H. G. Wilkens,[30] J. Z. Will,[99] H. H. Williams,[121] S. Williams,[28] C. Willis,[89] S. Willocq,[85] A. Wilson,[88] J.A. Wilson,[18] I. Wingerter-Seez,[5] F. Winklmeier,[115] B. T. Winter,[21] M. Wittgen,[144] T. Wittig,[43] J. Wittkowski,[99] S. J. Wollstadt,[82] M. W. Wolter,[39] H. Wolters,[125a,125c] B. K. Wosiek,[39] J. Wotschack,[30] M. J. Woudstra,[83] K. W. Wozniak,[39] M. Wright,[53] M. Wu,[55] S. L. Wu,[174] X. Wu,[49] Y. Wu,[88] E. Wulf,[35] T. R. Wyatt,[83] B. M. Wynne,[46] S. Xella,[36] M. Xiao,[137] D. Xu,[33a] L. Xu,[33b,ap] B. Yabsley,[151] S. Yacoob,[146b,aq] R. Yakabe,[66] M. Yamada,[65] H. Yamaguchi,[156] Y. Yamaguchi,[117] A. Yamamoto,[65] K. Yamamoto,[63] S. Yamamoto,[156] T. Yamamura,[156] T. Yamanaka,[156] K. Yamauchi,[102] Y. Yamazaki,[66] Z. Yan,[22] H. Yang,[33e] H. Yang,[174] U. K. Yang,[83] Y. Yang,[110] S. Yanush,[92] L. Yao,[33a] W-M. Yao,[15] Y. Yasu,[65] E. Yatsenko,[42] K. H. Yau Wong,[21] J. Ye,[40] S. Ye,[25] I. Yeletskikh,[64] A. L. Yen,[57] E. Yildirim,[42] M. Yilmaz,[4b] R. Yoosoofmiya,[124] K. Yorita,[172] R. Yoshida,[6] K. Yoshihara,[156] C. Young,[144] C. J. S. Young,[30] S. Youssef,[22] D. R. Yu,[15] J. Yu,[8] J. M. Yu,[88] J. Yu,[113] L. Yuan,[66] A. Yurkewicz,[107] I. Yusuff,[28,ar] B. Zabinski,[39] R. Zaidan,[62] A. M. Zaitsev,[129,ae] A. Zaman,[149] S. Zambito,[23] L. Zanello,[133a,133b] D. Zanzi,[100] C. Zeitnitz,[176] M. Zeman,[127] A. Zemla,[38a] K. Zengel,[23] O. Zenin,[129] T. Ženiš,[145a] D. Zerwas,[116] G. Zevi della Porta,[57] D. Zhang,[88] F. Zhang,[174] H. Zhang,[89] J. Zhang,[6] L. Zhang,[152] X. Zhang,[33d] Z. Zhang,[116] Z. Zhao,[33b] A. Zhemchugov,[64] J. Zhong,[119] B. Zhou,[88] L. Zhou,[35] N. Zhou,[164] C. G. Zhu,[33d] H. Zhu,[33a] J. Zhu,[88] Y. Zhu,[33b] X. Zhuang,[33a] K. Zhukov,[95] A. Zibell,[175] D. Zieminska,[60] N. I. Zimine,[64] C. Zimmermann,[82] R. Zimmermann,[21] S. Zimmermann,[21] S. Zimmermann,[48] Z. Zinonos,[54] M. Ziolkowski,[142] G. Zobernig,[174] A. Zoccoli,[20a,20b] M. zur Nedden,[16] G. Zurzolo,[103a,103b] V. Zutshi,[107] and L. Zwalinski[30]

(The ATLAS Collaboration)

[1]*Department of Physics, University of Adelaide, Adelaide, Australia*
[2]*Physics Department, SUNY Albany, Albany NY, United States of America*
[3]*Department of Physics, University of Alberta, Edmonton AB, Canada*
[4a]*Department of Physics, Ankara University, Ankara, Turkey*
[4b]*Department of Physics, Gazi University, Ankara, Turkey*
[4c]*Division of Physics, TOBB University of Economics and Technology, Ankara, Turkey*
[4d]*Turkish Atomic Energy Authority, Ankara, Turkey*
[5]*LAPP, CNRS/IN2P3 and Université Savoie Mont Blanc, Annecy-le-Vieux, France*
[6]*High Energy Physics Division, Argonne National Laboratory, Argonne IL, United States of America*

[7]*Department of Physics, University of Arizona, Tucson AZ, United States of America*

[8]*Department of Physics, The University of Texas at Arlington, Arlington TX, United States of America*

[9]*Physics Department, University of Athens, Athens, Greece*

[10]*Physics Department, National Technical University of Athens, Zografou, Greece*

[11]*Institute of Physics, Azerbaijan Academy of Sciences, Baku, Azerbaijan*

[12]*Institut de Física d'Altes Energies and Departament de Física de la Universitat Autònoma de Barcelona, Barcelona, Spain*

[13]*Institute of Physics, University of Belgrade, Belgrade, Serbia*

[14]*Department for Physics and Technology, University of Bergen, Bergen, Norway*

[15]*Physics Division, Lawrence Berkeley National Laboratory and University of California, Berkeley CA, United States of America*

[16]*Department of Physics, Humboldt University, Berlin, Germany*

[17]*Albert Einstein Center for Fundamental Physics and Laboratory for High Energy Physics, University of Bern, Bern, Switzerland*

[18]*School of Physics and Astronomy, University of Birmingham, Birmingham, United Kingdom*

[19a]*Department of Physics, Bogazici University, Istanbul, Turkey*

[19b]*Department of Physics, Dogus University, Istanbul, Turkey*

[19c]*Department of Physics Engineering, Gaziantep University, Gaziantep, Turkey*

[20a]*INFN Sezione di Bologna, Bologna, Italy*

[20b]*Dipartimento di Fisica e Astronomia, Università di Bologna, Bologna, Italy*

[21]*Physikalisches Institut, University of Bonn, Bonn, Germany*

[22]*Department of Physics, Boston University, Boston MA, United States of America*

[23]*Department of Physics, Brandeis University, Waltham MA, United States of America*

[24a]*Universidade Federal do Rio De Janeiro COPPE/EE/IF, Rio de Janeiro, Brazil*

[24b]*Electrical Circuits Department, Federal University of Juiz de Fora (UFJF), Juiz de Fora, Brazil*

[24c]*Federal University of Sao Joao del Rei (UFSJ), Sao Joao del Rei, Brazil*

[24d]*Instituto de Fisica, Universidade de Sao Paulo, Sao Paulo, Brazil*

[25]*Physics Department, Brookhaven National Laboratory, Upton NY, United States of America*

[26a]*National Institute of Physics and Nuclear Engineering, Bucharest, Romania*

[26b]*National Institute for Research and Development of Isotopic and Molecular Technologies, Physics Department, Cluj Napoca, Romania*

[26c]*University Politehnica Bucharest, Bucharest, Romania*

[26d]*West University in Timisoara, Timisoara, Romania*

[27]*Departamento de Física, Universidad de Buenos Aires, Buenos Aires, Argentina*

[28]*Cavendish Laboratory, University of Cambridge, Cambridge, United Kingdom*

[29]*Department of Physics, Carleton University, Ottawa ON, Canada*

[30]*CERN, Geneva, Switzerland*

[31]*Enrico Fermi Institute, University of Chicago, Chicago IL, United States of America*

[32a]*Departamento de Física, Pontificia Universidad Católica de Chile, Santiago, Chile*

[32b]*Departamento de Física, Universidad Técnica Federico Santa María, Valparaíso, Chile*

[33a]*Institute of High Energy Physics, Chinese Academy of Sciences, Beijing, China*

[33b]*Department of Modern Physics, University of Science and Technology of China, Anhui, China*

[33c]*Department of Physics, Nanjing University, Jiangsu, China*

[33d]*School of Physics, Shandong University, Shandong, China*

[33e]*Department of Physics and Astronomy, Shanghai Key Laboratory for Particle Physics and Cosmology, Shanghai Jiao Tong University, Shanghai, China*

[34]*Laboratoire de Physique Corpusculaire, Clermont Université and Université Blaise Pascal and CNRS/IN2P3, Clermont-Ferrand, France*

[35]*Nevis Laboratory, Columbia University, Irvington NY, United States of America*

[36]*Niels Bohr Institute, University of Copenhagen, Kobenhavn, Denmark*

[37a]*INFN Gruppo Collegato di Cosenza, Laboratori Nazionali di Frascati, Italy*

[37b]*Dipartimento di Fisica, Università della Calabria, Rende, Italy*

[38a]*AGH University of Science and Technology, Faculty of Physics and Applied Computer Science, Krakow, Poland*

[38b]*Marian Smoluchowski Institute of Physics, Jagiellonian University, Krakow, Poland*

[39]*Institute of Nuclear Physics Polish Academy of Sciences, Krakow, Poland*

[40]*Physics Department, Southern Methodist University, Dallas TX, United States of America*

[41]*Physics Department, University of Texas at Dallas, Richardson TX, United States of America*

[42]*DESY, Hamburg and Zeuthen, Germany*

[43]*Institut für Experimentelle Physik IV, Technische Universität Dortmund, Dortmund, Germany*

[44]*Institut für Kern- und Teilchenphysik, Technische Universität Dresden, Dresden, Germany*

[45]*Department of Physics, Duke University, Durham NC, United States of America*

[46]*SUPA - School of Physics and Astronomy, University of Edinburgh, Edinburgh, United Kingdom*

[47]*INFN Laboratori Nazionali di Frascati, Frascati, Italy*

[48]*Fakultät für Mathematik und Physik, Albert-Ludwigs-Universität, Freiburg, Germany*

[49]*Section de Physique, Université de Genève, Geneva, Switzerland*
[50a]*INFN Sezione di Genova, Genova, Italy*
[50b]*Dipartimento di Fisica, Università di Genova, Genova, Italy*
[51a]*E. Andronikashvili Institute of Physics, Iv. Javakhishvili Tbilisi State University, Tbilisi, Georgia*
[51b]*High Energy Physics Institute, Tbilisi State University, Tbilisi, Georgia*
[52]*II Physikalisches Institut, Justus-Liebig-Universität Giessen, Giessen, Germany*
[53]*SUPA - School of Physics and Astronomy, University of Glasgow, Glasgow, United Kingdom*
[54]*II Physikalisches Institut, Georg-August-Universität, Göttingen, Germany*
[55]*Laboratoire de Physique Subatomique et de Cosmologie, Université Grenoble-Alpes, CNRS/IN2P3, Grenoble, France*
[56]*Department of Physics, Hampton University, Hampton VA, United States of America*
[57]*Laboratory for Particle Physics and Cosmology, Harvard University, Cambridge MA, United States of America*
[58a]*Kirchhoff-Institut für Physik, Ruprecht-Karls-Universität Heidelberg, Heidelberg, Germany*
[58b]*Physikalisches Institut, Ruprecht-Karls-Universität Heidelberg, Heidelberg, Germany*
[58c]*ZITI Institut für technische Informatik, Ruprecht-Karls-Universität Heidelberg, Mannheim, Germany*
[59]*Faculty of Applied Information Science, Hiroshima Institute of Technology, Hiroshima, Japan*
[60]*Department of Physics, Indiana University, Bloomington IN, United States of America*
[61]*Institut für Astro- und Teilchenphysik, Leopold-Franzens-Universität, Innsbruck, Austria*
[62]*University of Iowa, Iowa City IA, United States of America*
[63]*Department of Physics and Astronomy, Iowa State University, Ames IA, United States of America*
[64]*Joint Institute for Nuclear Research, JINR Dubna, Dubna, Russia*
[65]*KEK, High Energy Accelerator Research Organization, Tsukuba, Japan*
[66]*Graduate School of Science, Kobe University, Kobe, Japan*
[67]*Faculty of Science, Kyoto University, Kyoto, Japan*
[68]*Kyoto University of Education, Kyoto, Japan*
[69]*Department of Physics, Kyushu University, Fukuoka, Japan*
[70]*Instituto de Física La Plata, Universidad Nacional de La Plata and CONICET, La Plata, Argentina*
[71]*Physics Department, Lancaster University, Lancaster, United Kingdom*
[72a]*INFN Sezione di Lecce, Lecce, Italy*
[72b]*Dipartimento di Matematica e Fisica, Università del Salento, Lecce, Italy*
[73]*Oliver Lodge Laboratory, University of Liverpool, Liverpool, United Kingdom*
[74]*Department of Physics, Jožef Stefan Institute and University of Ljubljana, Ljubljana, Slovenia*
[75]*School of Physics and Astronomy, Queen Mary University of London, London, United Kingdom*
[76]*Department of Physics, Royal Holloway University of London, Surrey, United Kingdom*
[77]*Department of Physics and Astronomy, University College London, London, United Kingdom*
[78]*Louisiana Tech University, Ruston LA, United States of America*
[79]*Laboratoire de Physique Nucléaire et de Hautes Energies, UPMC and Université Paris-Diderot and CNRS/IN2P3, Paris, France*
[80]*Fysiska institutionen, Lunds universitet, Lund, Sweden*
[81]*Departamento de Fisica Teorica C-15, Universidad Autonoma de Madrid, Madrid, Spain*
[82]*Institut für Physik, Universität Mainz, Mainz, Germany*
[83]*School of Physics and Astronomy, University of Manchester, Manchester, United Kingdom*
[84]*CPPM, Aix-Marseille Université and CNRS/IN2P3, Marseille, France*
[85]*Department of Physics, University of Massachusetts, Amherst MA, United States of America*
[86]*Department of Physics, McGill University, Montreal QC, Canada*
[87]*School of Physics, University of Melbourne, Victoria, Australia*
[88]*Department of Physics, The University of Michigan, Ann Arbor MI, United States of America*
[89]*Department of Physics and Astronomy, Michigan State University, East Lansing MI, United States of America*
[90a]*INFN Sezione di Milano, Milano, Italy*
[90b]*Dipartimento di Fisica, Università di Milano, Milano, Italy*
[91]*B.I. Stepanov Institute of Physics, National Academy of Sciences of Belarus, Minsk, Republic of Belarus*
[92]*National Scientific and Educational Centre for Particle and High Energy Physics, Minsk, Republic of Belarus*
[93]*Department of Physics, Massachusetts Institute of Technology, Cambridge MA, United States of America*
[94]*Group of Particle Physics, University of Montreal, Montreal QC, Canada*
[95]*P.N. Lebedev Institute of Physics, Academy of Sciences, Moscow, Russia*
[96]*Institute for Theoretical and Experimental Physics (ITEP), Moscow, Russia*
[97]*National Research Nuclear University MEPhI, Moscow, Russia*
[98]*D.V. Skobeltsyn Institute of Nuclear Physics, M.V. Lomonosov Moscow State University, Moscow, Russia*
[99]*Fakultät für Physik, Ludwig-Maximilians-Universität München, München, Germany*
[100]*Max-Planck-Institut für Physik (Werner-Heisenberg-Institut), München, Germany*
[101]*Nagasaki Institute of Applied Science, Nagasaki, Japan*

[102]*Graduate School of Science and Kobayashi-Maskawa Institute, Nagoya University, Nagoya, Japan*

[103a]*INFN Sezione di Napoli, Napoli, Italy*

[103b]*Dipartimento di Fisica, Università di Napoli, Napoli, Italy*

[104]*Department of Physics and Astronomy, University of New Mexico, Albuquerque NM, United States of America*

[105]*Institute for Mathematics, Astrophysics and Particle Physics, Radboud University Nijmegen/Nikhef, Nijmegen, Netherlands*

[106]*Nikhef National Institute for Subatomic Physics and University of Amsterdam, Amsterdam, Netherlands*

[107]*Department of Physics, Northern Illinois University, DeKalb IL, United States of America*

[108]*Budker Institute of Nuclear Physics, SB RAS, Novosibirsk, Russia*

[109]*Department of Physics, New York University, New York NY, United States of America*

[110]*Ohio State University, Columbus OH, United States of America*

[111]*Faculty of Science, Okayama University, Okayama, Japan*

[112]*Homer L. Dodge Department of Physics and Astronomy, University of Oklahoma, Norman OK, United States of America*

[113]*Department of Physics, Oklahoma State University, Stillwater OK, United States of America*

[114]*Palacký University, RCPTM, Olomouc, Czech Republic*

[115]*Center for High Energy Physics, University of Oregon, Eugene OR, United States of America*

[116]*LAL, Université Paris-Sud and CNRS/IN2P3, Orsay, France*

[117]*Graduate School of Science, Osaka University, Osaka, Japan*

[118]*Department of Physics, University of Oslo, Oslo, Norway*

[119]*Department of Physics, Oxford University, Oxford, United Kingdom*

[120a]*INFN Sezione di Pavia, Pavia, Italy*

[120b]*Dipartimento di Fisica, Università di Pavia, Pavia, Italy*

[121]*Department of Physics, University of Pennsylvania, Philadelphia PA, United States of America*

[122]*National Research Centre "Kurchatov Institute" B.P.Konstantinov Petersburg Nuclear Physics Institute, St. Petersburg, Russia*

[123a]*INFN Sezione di Pisa, Pisa, Italy*

[123b]*Dipartimento di Fisica E. Fermi, Università di Pisa, Pisa, Italy*

[124]*Department of Physics and Astronomy, University of Pittsburgh, Pittsburgh PA, United States of America*

[125a]*Laboratório de Instrumentação e Física Experimental de Partículas - LIP, Lisboa, Portugal*

[125b]*Faculdade de Ciências, Universidade de Lisboa, Lisboa, Portugal*

[125c]*Department of Physics, University of Coimbra, Coimbra, Portugal*

[125d]*Centro de Física Nuclear da Universidade de Lisboa, Lisboa, Portugal*

[125e]*Departamento de Fisica, Universidade do Minho, Braga, Portugal*

[125f]*Departamento de Fisica Teorica y del Cosmos and CAFPE, Universidad de Granada, Granada (Spain), Portugal*

[125g]*Dep Fisica and CEFITEC of Faculdade de Ciencias e Tecnologia, Universidade Nova de Lisboa, Caparica, Portugal*

[126]*Institute of Physics, Academy of Sciences of the Czech Republic, Praha, Czech Republic*

[127]*Czech Technical University in Prague, Praha, Czech Republic*

[128]*Faculty of Mathematics and Physics, Charles University in Prague, Praha, Czech Republic*

[129]*State Research Center Institute for High Energy Physics, Protvino, Russia*

[130]*Particle Physics Department, Rutherford Appleton Laboratory, Didcot, United Kingdom*

[131]*Physics Department, University of Regina, Regina SK, Canada*

[132]*Ritsumeikan University, Kusatsu, Shiga, Japan*

[133a]*INFN Sezione di Roma, Roma, Italy*

[133b]*Dipartimento di Fisica, Sapienza Università di Roma, Roma, Italy*

[134a]*INFN Sezione di Roma Tor Vergata, Roma, Italy*

[134b]*Dipartimento di Fisica, Università di Roma Tor Vergata, Roma, Italy*

[135a]*INFN Sezione di Roma Tre, Roma, Italy*

[135b]*Dipartimento di Matematica e Fisica, Università Roma Tre, Roma, Italy*

[136a]*Faculté des Sciences Ain Chock, Réseau Universitaire de Physique des Hautes Energies - Université Hassan II, Casablanca, Morocco*

[136b]*Centre National de l'Energie des Sciences Techniques Nucleaires, Rabat, Morocco*

[136c]*Faculté des Sciences Semlalia, Université Cadi Ayyad, LPHEA-Marrakech, Morocco*

[136d]*Faculté des Sciences, Université Mohamed Premier and LPTPM, Oujda, Morocco*

[136e]*Faculté des sciences, Université Mohammed V-Agdal, Rabat, Morocco*

[137]*DSM/IRFU (Institut de Recherches sur les Lois Fondamentales de l'Univers), CEA Saclay (Commissariat à l'Energie Atomique et aux Energies Alternatives), Gif-sur-Yvette, France*

[138]*Santa Cruz Institute for Particle Physics, University of California Santa Cruz, Santa Cruz CA, United States of America*

[139]*Department of Physics, University of Washington, Seattle WA, United States of America*

[140]*Department of Physics and Astronomy, University of Sheffield, Sheffield, United Kingdom*

[141]*Department of Physics, Shinshu University, Nagano, Japan*

[142]*Fachbereich Physik, Universität Siegen, Siegen, Germany*

[143]*Department of Physics, Simon Fraser University, Burnaby BC, Canada*

[144]*SLAC National Accelerator Laboratory, Stanford CA, United States of America*

[145a]*Faculty of Mathematics, Physics & Informatics, Comenius University, Bratislava, Slovak Republic*

[145b]*Department of Subnuclear Physics, Institute of Experimental Physics of the Slovak Academy of Sciences, Kosice, Slovak Republic*

[146a]*Department of Physics, University of Cape Town, Cape Town, South Africa*

[146b]*Department of Physics, University of Johannesburg, Johannesburg, South Africa*

[146c]*School of Physics, University of the Witwatersrand, Johannesburg, South Africa*

[147a]*Department of Physics, Stockholm University, Stockholm, Sweden*

[147b]*The Oskar Klein Centre, Stockholm, Sweden*

[148]*Physics Department, Royal Institute of Technology, Stockholm, Sweden*

[149]*Departments of Physics & Astronomy and Chemistry, Stony Brook University, Stony Brook NY, United States of America*

[150]*Department of Physics and Astronomy, University of Sussex, Brighton, United Kingdom*

[151]*School of Physics, University of Sydney, Sydney, Australia*

[152]*Institute of Physics, Academia Sinica, Taipei, Taiwan*

[153]*Department of Physics, Technion: Israel Institute of Technology, Haifa, Israel*

[154]*Raymond and Beverly Sackler School of Physics and Astronomy, Tel Aviv University, Tel Aviv, Israel*

[155]*Department of Physics, Aristotle University of Thessaloniki, Thessaloniki, Greece*

[156]*International Center for Elementary Particle Physics and Department of Physics, The University of Tokyo, Tokyo, Japan*

[157]*Graduate School of Science and Technology, Tokyo Metropolitan University, Tokyo, Japan*

[158]*Department of Physics, Tokyo Institute of Technology, Tokyo, Japan*

[159]*Department of Physics, University of Toronto, Toronto ON, Canada*

[160a]*TRIUMF, Vancouver BC, Canada*

[160b]*Department of Physics and Astronomy, York University, Toronto ON, Canada*

[161]*Faculty of Pure and Applied Sciences, University of Tsukuba, Tsukuba, Japan*

[162]*Department of Physics and Astronomy, Tufts University, Medford MA, United States of America*

[163]*Centro de Investigaciones, Universidad Antonio Narino, Bogota, Colombia*

[164]*Department of Physics and Astronomy, University of California Irvine, Irvine CA, United States of America*

[165a]*INFN Gruppo Collegato di Udine, Sezione di Trieste, Udine*

[165b]*ICTP, Trieste, Italy*

[165c]*Dipartimento di Chimica, Fisica e Ambiente, Università di Udine, Udine, Italy*

[166]*Department of Physics, University of Illinois, Urbana IL, United States of America*

[167]*Department of Physics and Astronomy, University of Uppsala, Uppsala, Sweden*

[168]*Instituto de Física Corpuscular (IFIC) and Departamento de Física Atómica, Molecular y Nuclear and Departamento de Ingeniería Electrónica and Instituto de Microelectrónica de Barcelona (IMB-CNM), University of Valencia and CSIC, Valencia, Spain*

[169]*Department of Physics, University of British Columbia, Vancouver BC, Canada*

[170]*Department of Physics and Astronomy, University of Victoria, Victoria BC, Canada*

[171]*Department of Physics, University of Warwick, Coventry, United Kingdom*

[172]*Waseda University, Tokyo, Japan*

[173]*Department of Particle Physics, The Weizmann Institute of Science, Rehovot, Israel*

[174]*Department of Physics, University of Wisconsin, Madison WI, United States of America*

[175]*Fakultät für Physik und Astronomie, Julius-Maximilians-Universität, Würzburg, Germany*

[176]*Fachbereich C Physik, Bergische Universität Wuppertal, Wuppertal, Germany*

[177]*Department of Physics, Yale University, New Haven CT, United States of America*

[178]*Yerevan Physics Institute, Yerevan, Armenia*

[179]*Centre de Calcul de l'Institut National de Physique Nucléaire et de Physique des Particules (IN2P3), Villeurbanne, France*

[a]Also at Department of Physics, King's College London, London, United Kingdom

[b]Also at Institute of Physics, Azerbaijan Academy of Sciences, Baku, Azerbaijan

[c]Also at Novosibirsk State University, Novosibirsk, Russia

[d]Also at Particle Physics Department, Rutherford Appleton Laboratory, Didcot, United Kingdom

[e]Also at TRIUMF, Vancouver BC, Canada

[f]Also at Department of Physics, California State University, Fresno CA, United States of America

[g]Also at Department of Physics, University of Fribourg, Fribourg, Switzerland

[h]Also at Departamento de Fisica e Astronomia, Faculdade de Ciencias, Universidade do Porto, Portugal

[i]Also at Tomsk State University, Tomsk, Russia

[j]Also at CPPM, Aix-Marseille Université and CNRS/IN2P3, Marseille, France

[k]Also at Universita di Napoli Parthenope, Napoli, Italy

[l]Also at Institute of Particle Physics (IPP), Canada

[m]Also at Department of Physics, St. Petersburg State Polytechnical University, St. Petersburg, Russia

[n]Also at Chinese University of Hong Kong, China

[o]Also at Louisiana Tech University, Ruston LA, United States of America

[p]Also at Institucio Catalana de Recerca i Estudis Avancats, ICREA, Barcelona, Spain

[q]Also at Department of Physics, The University of Texas at Austin, Austin TX, United States of America

[r]Also at Institute of Theoretical Physics, Ilia State University, Tbilisi, Georgia

[s]Also at CERN, Geneva, Switzerland

[t]Also at Georgian Technical University (GTU),Tbilisi, Georgia

[u]Also at Ochadai Academic Production, Ochanomizu University, Tokyo, Japan

[v]Also at Manhattan College, New York NY, United States of America

[w]Also at Hellenic Open University, Patras, Greece

[x]Also at Institute of Physics, Academia Sinica, Taipei, Taiwan

[y]Also at LAL, Université Paris-Sud and CNRS/IN2P3, Orsay, France

[z]Also at Academia Sinica Grid Computing, Institute of Physics, Academia Sinica, Taipei, Taiwan

[aa]Also at School of Physics, Shandong University, Shandong, China

[ab]Also at Laboratoire de Physique Nucléaire et de Hautes Energies, UPMC and Université Paris-Diderot and CNRS/IN2P3, Paris, France

[ac]Also at School of Physical Sciences, National Institute of Science Education and Research, Bhubaneswar, India

[ad]Also at Dipartimento di Fisica, Sapienza Università di Roma, Roma, Italy

[ae]Also at Moscow Institute of Physics and Technology State University, Dolgoprudny, Russia

[af]Also at Section de Physique, Université de Genève, Geneva, Switzerland

[ag]Also at International School for Advanced Studies (SISSA), Trieste, Italy

[ah]Also at Department of Physics and Astronomy, University of South Carolina, Columbia SC, United States of America

[ai]Also at School of Physics and Engineering, Sun Yat-sen University, Guangzhou, China

[aj]Also at Faculty of Physics, M.V.Lomonosov Moscow State University, Moscow, Russia

[ak]Also at National Research Nuclear University MEPhI, Moscow, Russia

[al]Also at Institute for Particle and Nuclear Physics, Wigner Research Centre for Physics, Budapest, Hungary

[am]Also at Department of Physics, Oxford University, Oxford, United Kingdom

[an]Also at Department of Physics, Nanjing University, Jiangsu, China

[ao]Also at Institut für Experimentalphysik, Universität Hamburg, Hamburg, Germany

[ap]Also at Department of Physics, The University of Michigan, Ann Arbor MI, United States of America

[aq]Also at Discipline of Physics, University of KwaZulu-Natal, Durban, South Africa

[ar]Also at University of Malaya, Department of Physics, Kuala Lumpur, Malaysia

[*]Deceased